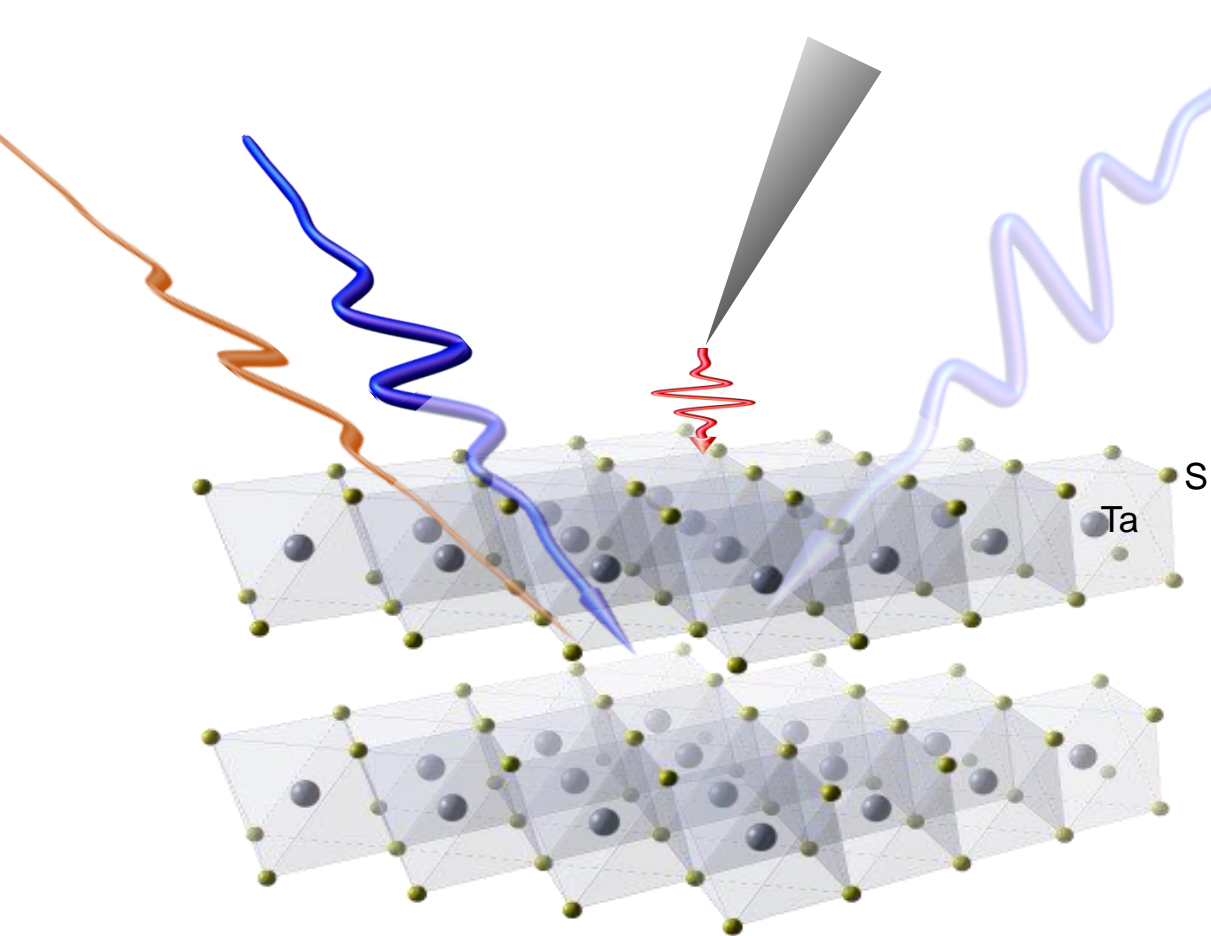


Exotic phenomena in a metastable polaronic Wigner crystal.



**Y. Vaskivskiy¹, A.Mraz¹, J.Vodeb¹, E. Božin², I. Vaskivsyi¹
and D. Mihailovic^{1,3,4}**

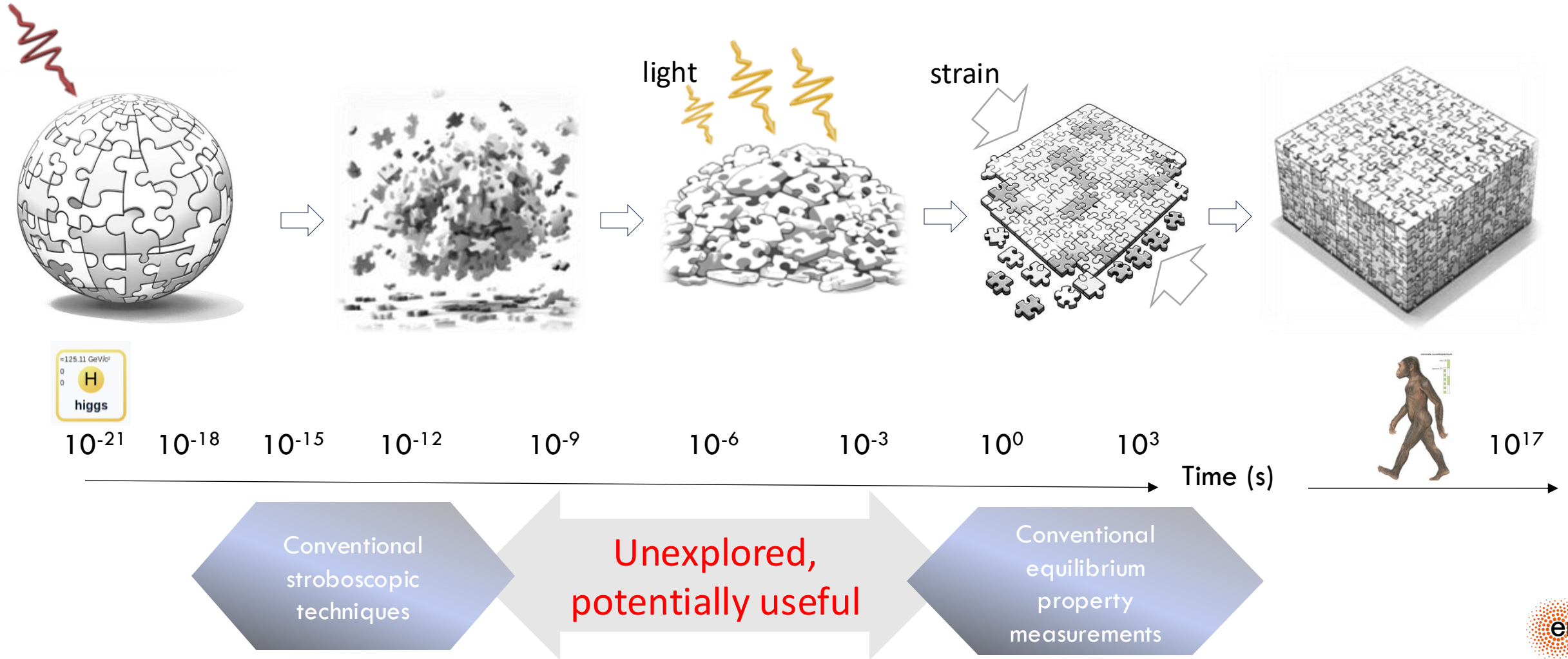
¹Jožef Stefan Institute, Jamova 39, Ljubljana, Slovenia,

²Brookhaven National Laboratory, Upton, N.Y., USA

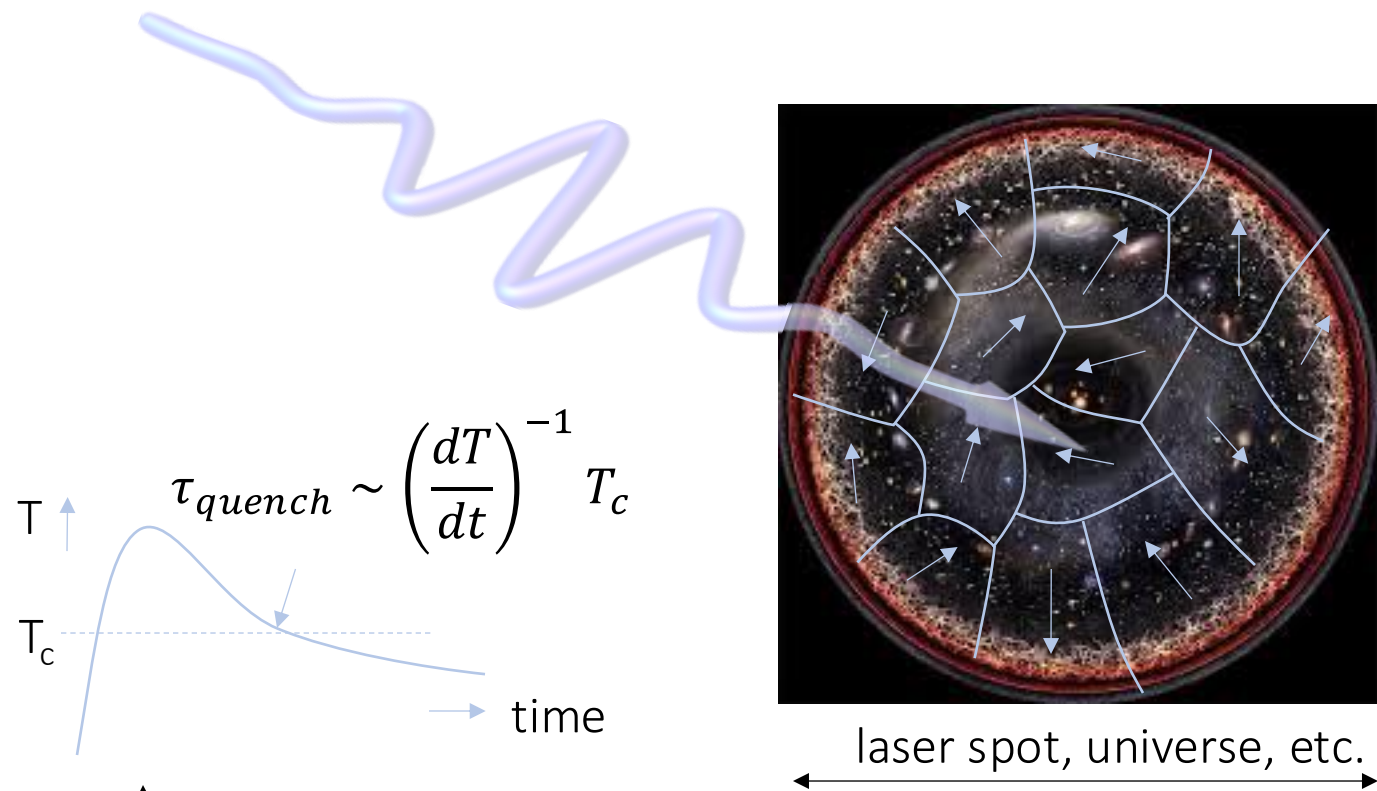
*³Department. of Physics, Faculty of Mathematics and
physics, University of Ljubljana, Slovenia*

⁴CENN Nanocenter, Jamova 30, 1000 Ljubljana, Slovenia

Mesoscopic states and metastability in the aftermath of a phase transition



Creation of metastable states by a quench through a 2nd order transition



whether as it expands and cools it might acquire a domain structure, as in a ferromagnet cooled through its Curie point. Zel'dovich *et al* (1974; see also Kobzarev *et al* 1974) have discussed this question, and in particular pointed out the important gravitational effects to be expected of domain walls. Everett (1974) has studied the propagation of waves across a domain boundary.

The aim of this paper is to discuss the topology and scale of the possible cosmological



T. Kibble, *J Phys a-Math Gen* **9**, 1387 (1976).

W. Zurek, *Nature* **317**, 505 (1985).

If $\tau_{quench} < L/v$, multiple domains form (Kibble-Zurek mechanism)

$$\Psi = Ae^{i\phi}$$

Possible single 1st order transition outcomes

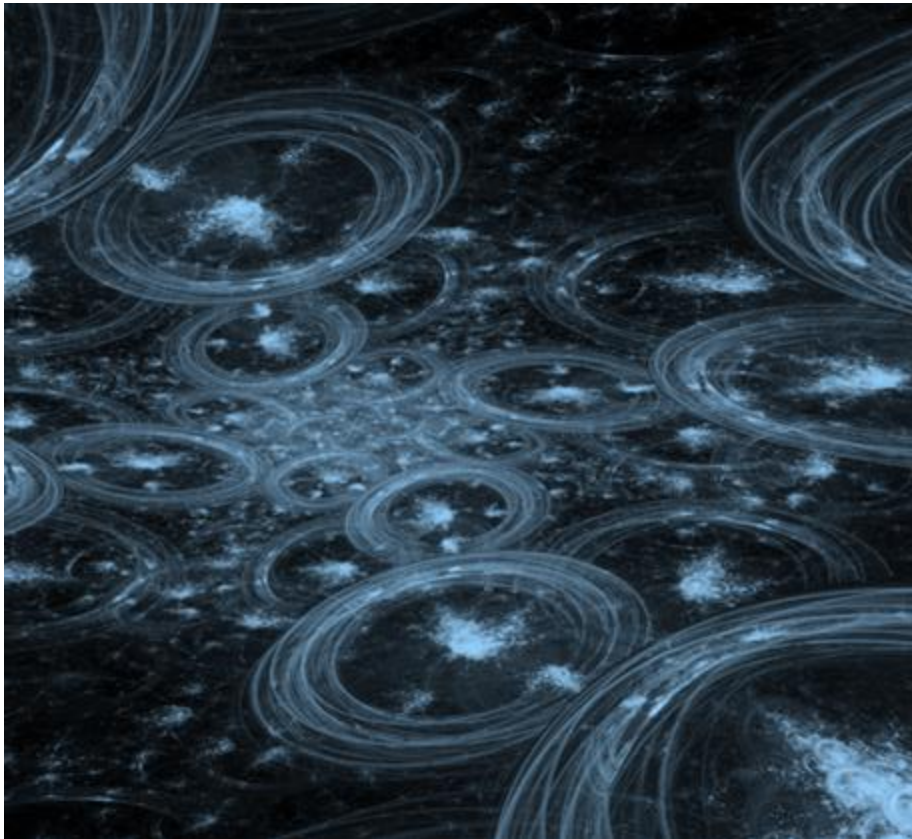
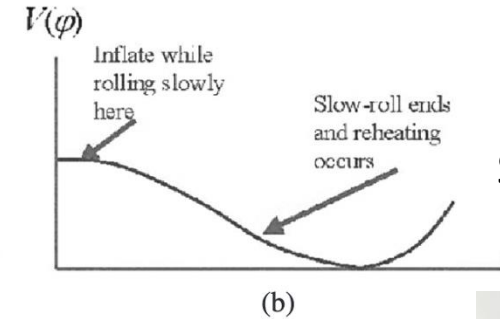
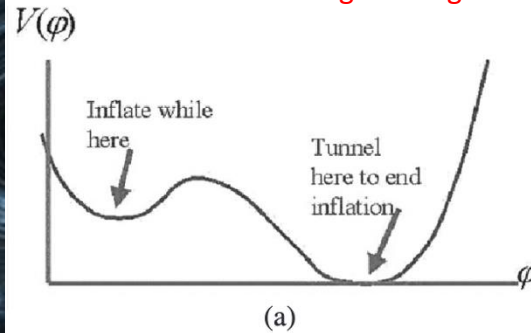
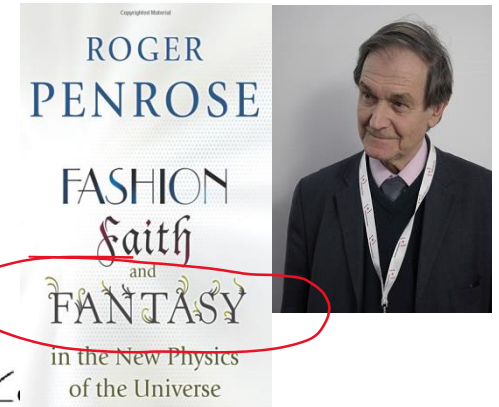
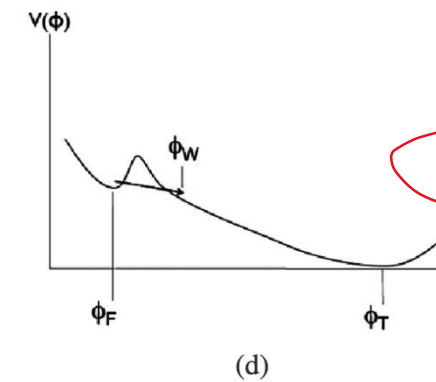
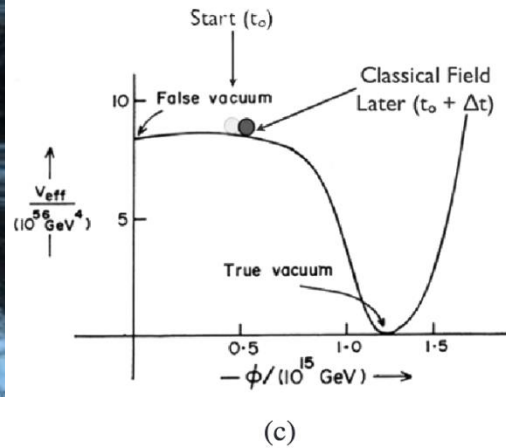


Figure: Roger Penrose's 'Fantasy'

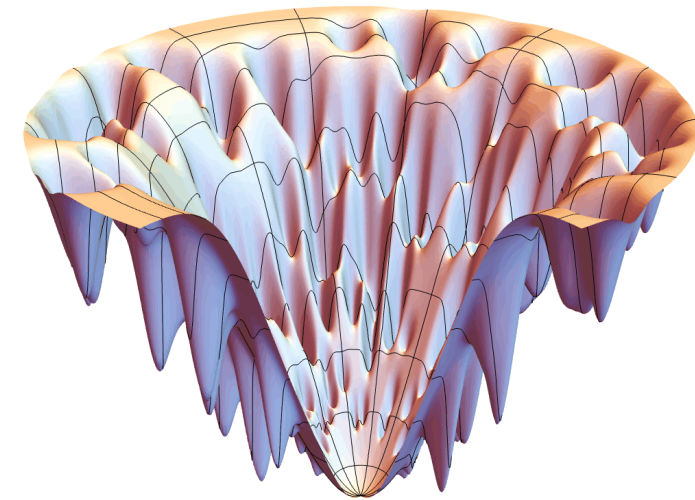
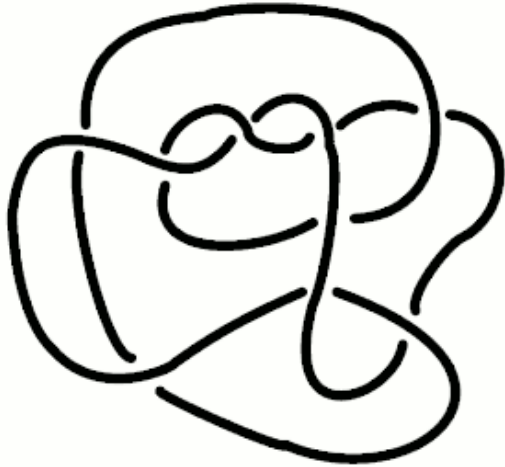


Starobinsky – Linde – Guth
Kibble, Zurek, Volovik



We have little data over a vast range of timescales!

An example of multiple outcomes: Protein folding



Vol 465 | 3 June 2010 | [nature](#) | [nature.com](#)

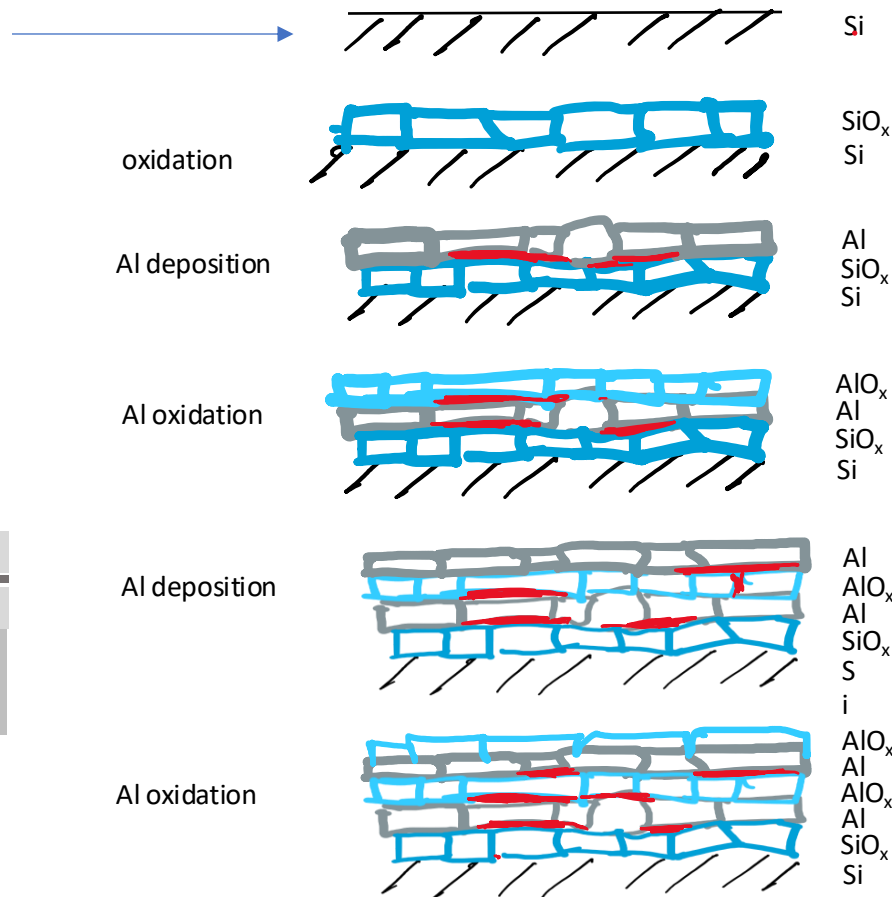
nature

LETTERS

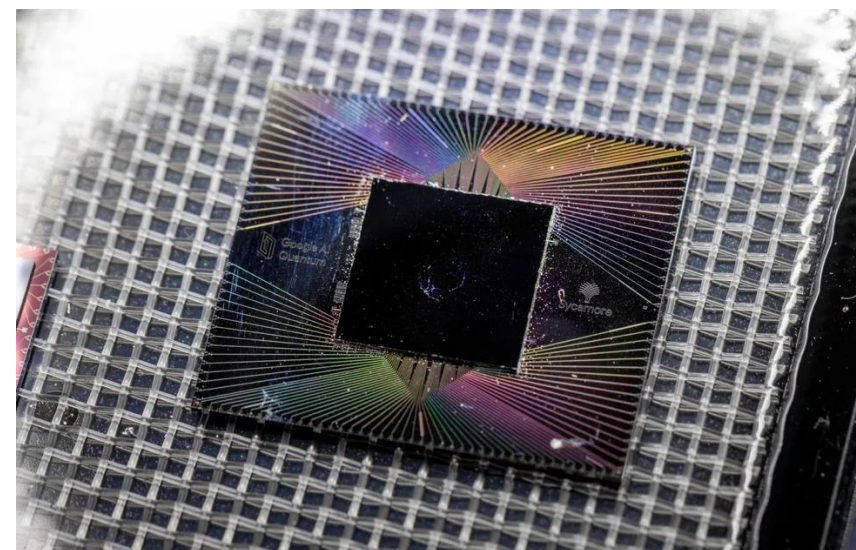
The folding cooperativity of a protein is controlled by its chain topology

Elizabeth A. Shank^{1,2*}†, Ciro Cecconi^{1,2*}†, Jesse W. Dill^{2,3*}, Susan Marqusee^{1,2} & Carlos Bustamante^{1,2,4,5,6}

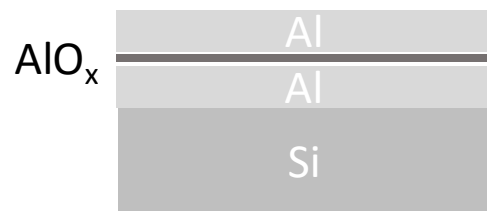
Superconducting QPU fabrication



The fabrication of a QPU typically requires ~40 steps



Ideal engineering view:



Optimization of Al/AIO_x/Al-layer systems for Josephson junctions from a microstructure point of view

Cite as: J. Appl. Phys. 125, 165301 (2019); doi:10.1063/1.5088871
 Submitted: 23 January 2019
 Published Online: 22 April 2019

S. Fritz,^{1,a)} L. Radtke,² R.

Al/Al_x/Al
 junctions
 different
 conditions

Processor	QPU status	Processor type	Qubits	EPLG	CLOPS
ibm_fez	Online	Heron r2	156	0.5%	3.8K
ibm_torino	Online	Heron r1	133	0.7%	3.8K
ibm_kyiv	Online	Eagle r3	127	1.9%	5K
ibm_quebec	Online	Eagle r3	127	2.6%	5K
ibm_sherbrooke	Online	Eagle r3	127	2.9%	5K
ibm_kyoto	Online	Eagle r3	127	2.9%	5K
ibm_brussels	Online	Eagle r3	127	3%	5K
ibm_kawasaki	Online	Eagle r3	127	3.2%	5K
ibm_rensseleer	Online	Eagle r3	127	3.8%	5K
ibm_strasbourg	Online	Eagle r3	127	3.9%	5K
ibm_nazca	Online	Eagle r3	127	4.1%	5K
ibm_brisbane	Online	Eagle r3	127	5.7%	5K

ibm_fez

OpenQASM 3

156

Status: ● Online

Median CZ error: 2.933e-3

Median SX error: 2.684e-4

Median readout error: 1.690e-2

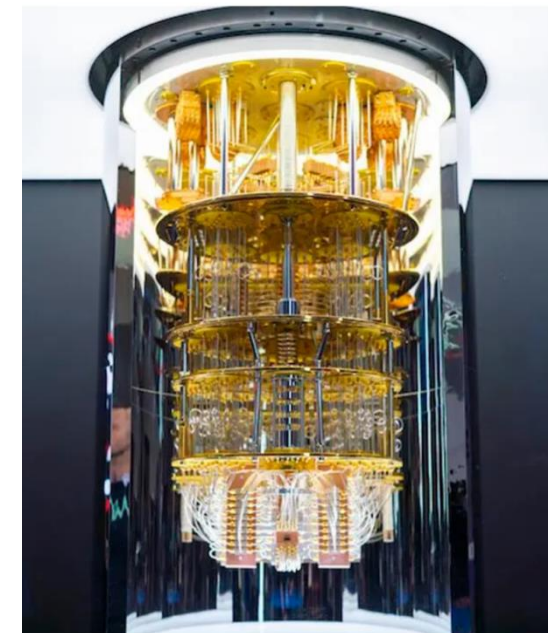
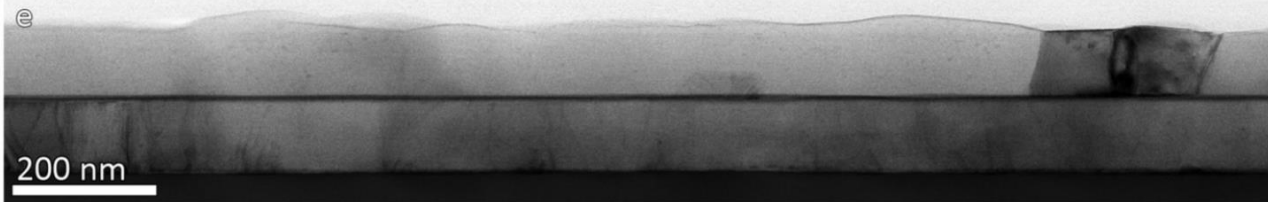
Median T1: 116.16 us

Median T2: 94.94 us

2 jobs

n r2

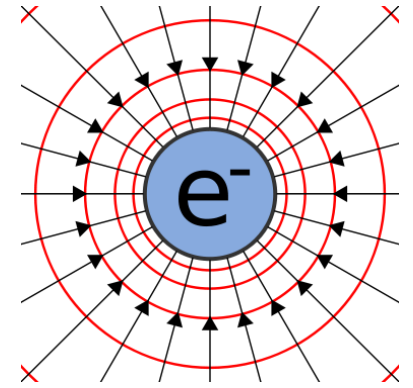
SX, X



IBM Q1

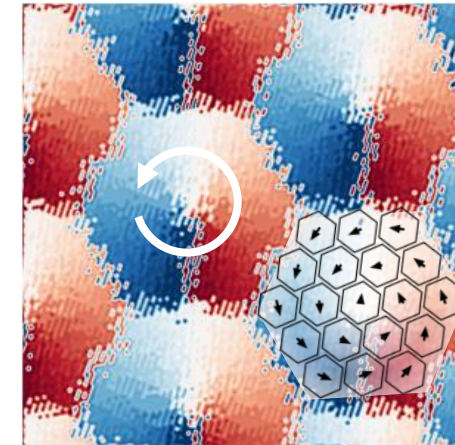
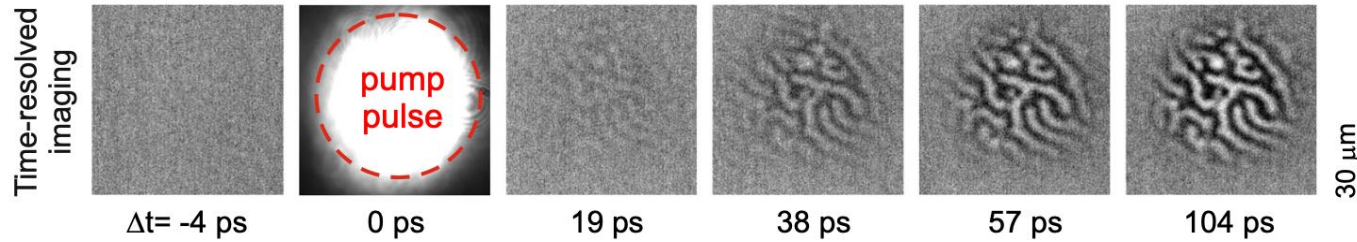


Domains store information (spin and charge)



Spins are weakly coupled to the environment, whence they hold information better than charge, but **information is encoded in the domain structure**

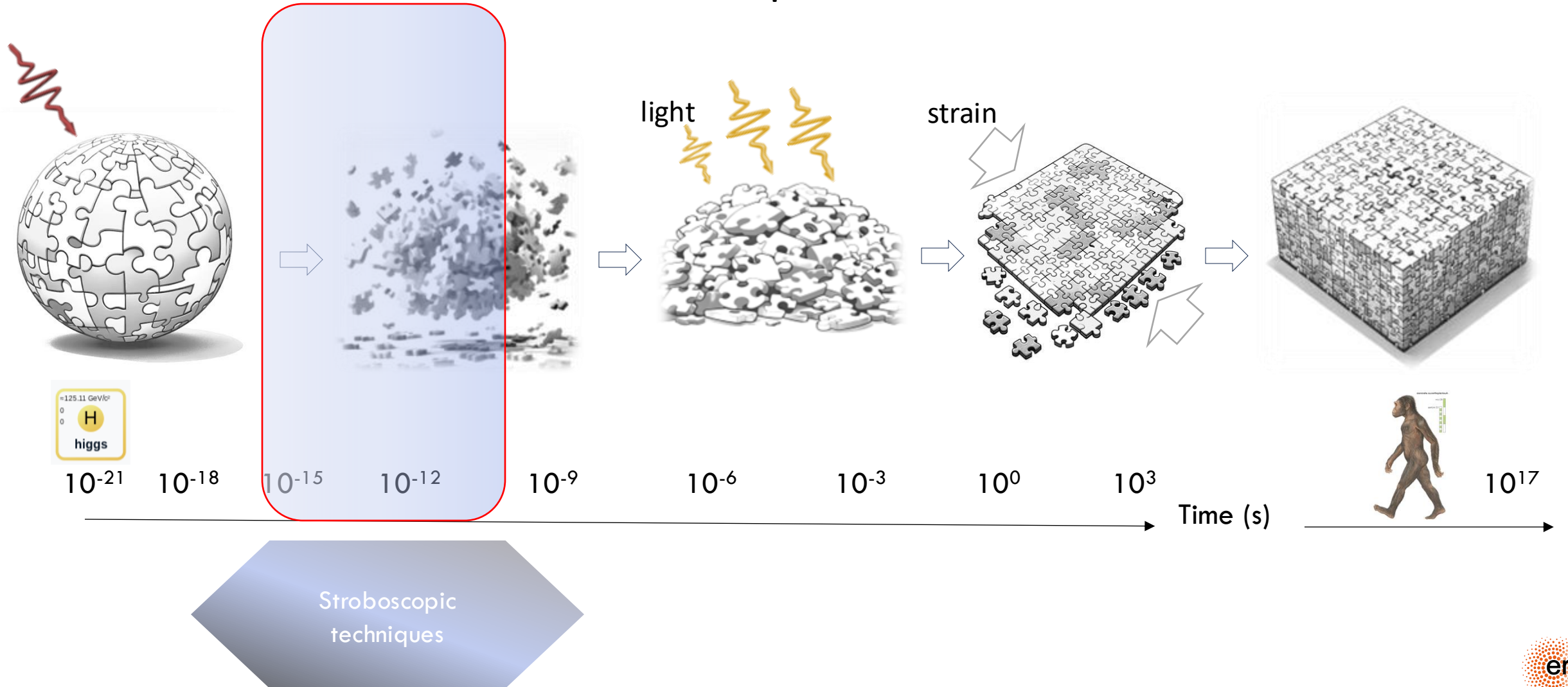
Charge is strongly coupled to the lattice, whence any information is rapidly dissipated.
But, information can be encoded in the domain structure.



de Jong *et al.* PRL**108**, (2012).
Nature Communications | (2024) 15:4451

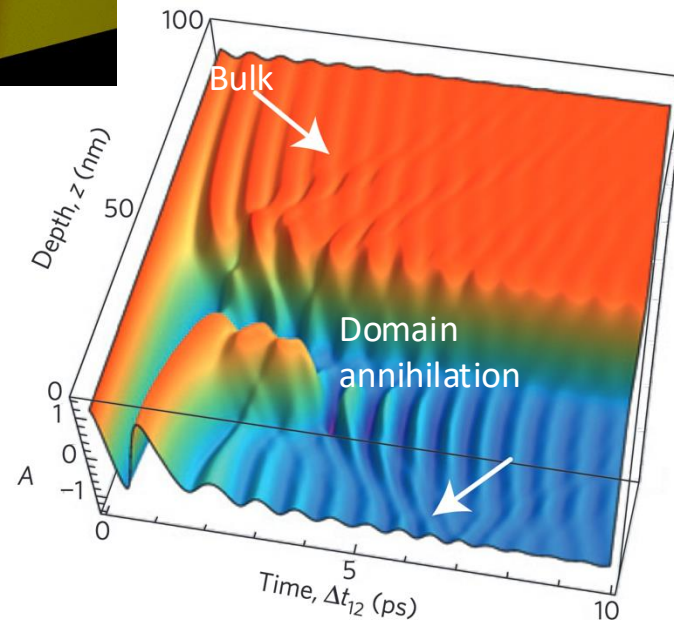
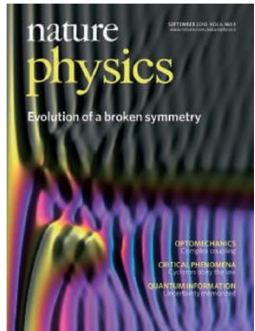
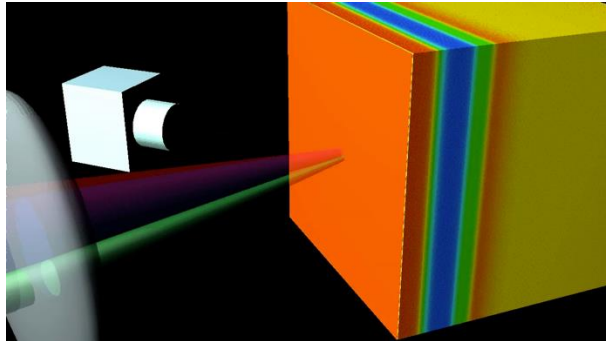
e.g. 1T-TaS2 memory (Mraz *et al.*, *Nanolett.* 2022)

Mesoscopic states and metastability in the aftermath of a phase transition

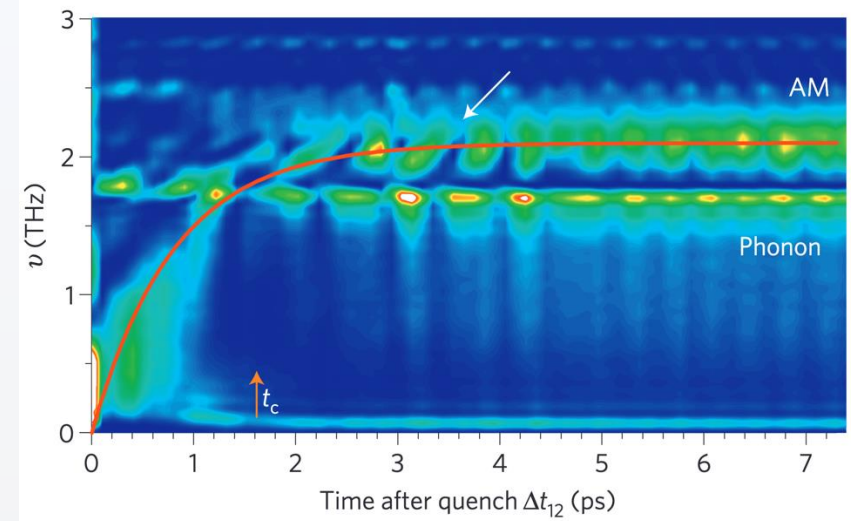


Coherent domain dynamics in TbTe_3

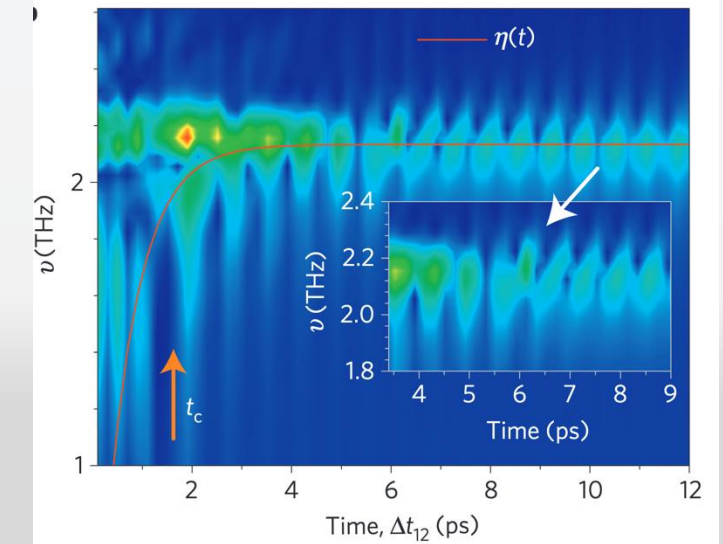
Domains form due to inhomogeneous excitation



Experiment



Theory



Yusupov, R. *et al.* Coherent dynamics of macroscopic electronic order through a symmetry breaking transition. *Nat Phys* **6**, 681–684 (2010).

Incoherent Topological Defect Recombination Dynamics in TbTe_3

T. Mertelj,¹ P. Kusar,¹ V. V. Kabanov,¹ P. Giraldo-Gallo,² I. R. Fisher,^{2,3} and D. Mihailovic^{1,4}

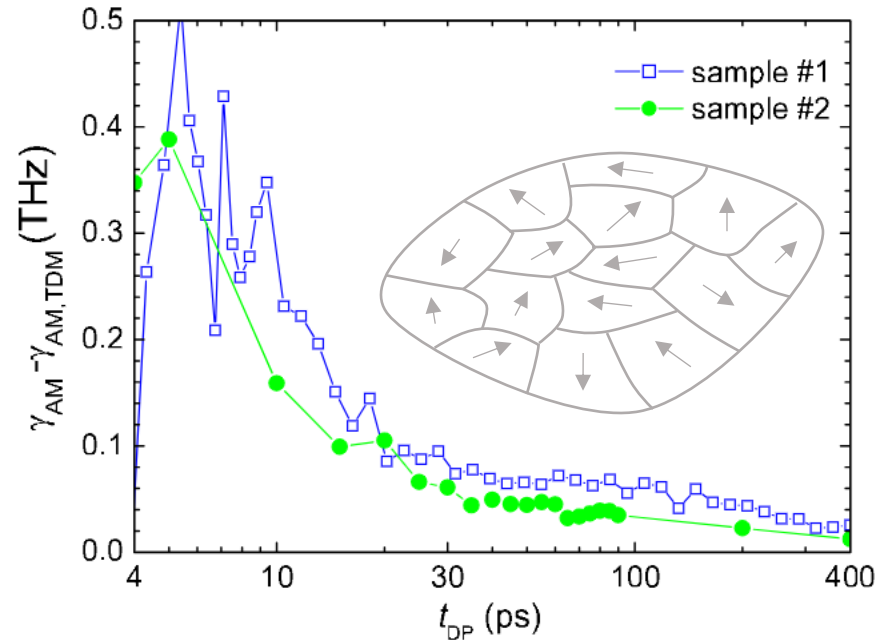


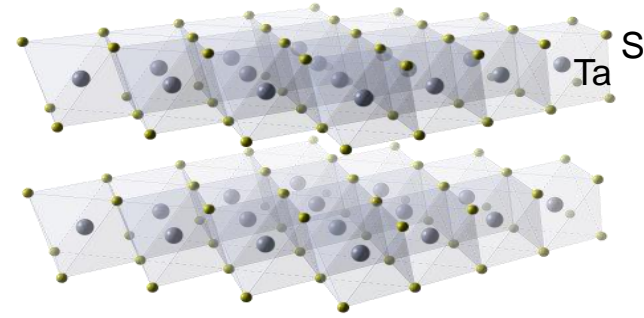
FIG. 4 (color online). The time dependence of the excess γ_{AM} due to topological defect annihilation. Data for two different samples show a difference primarily in the long time behavior beyond 30 ps, which appears as an offset.

See also Trigo et al (e.g. TR-XRD)

Ultrafast Switching to a Stable Hidden Quantum State in an Electronic Crystal

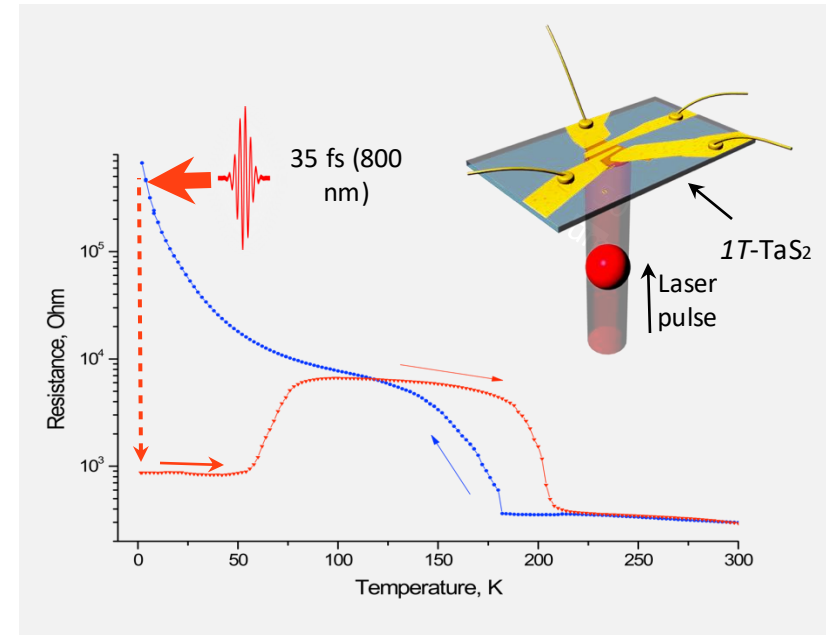
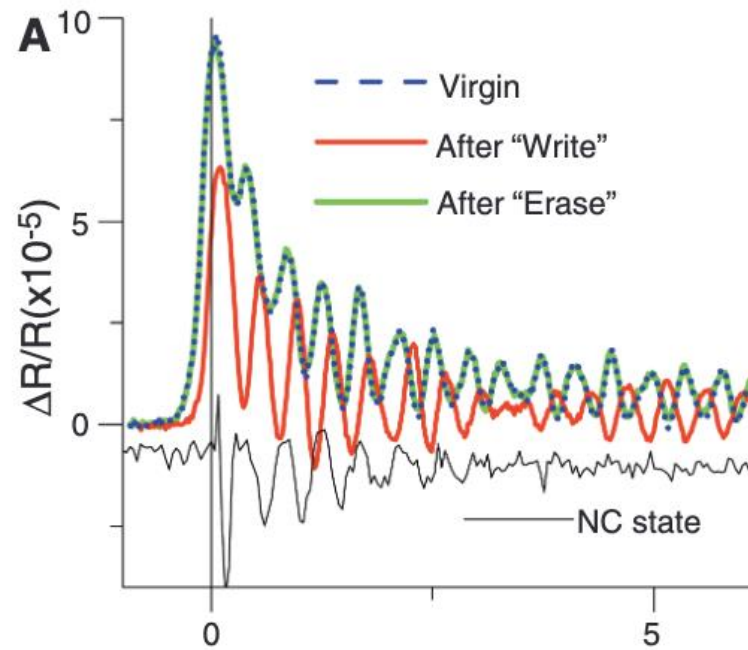
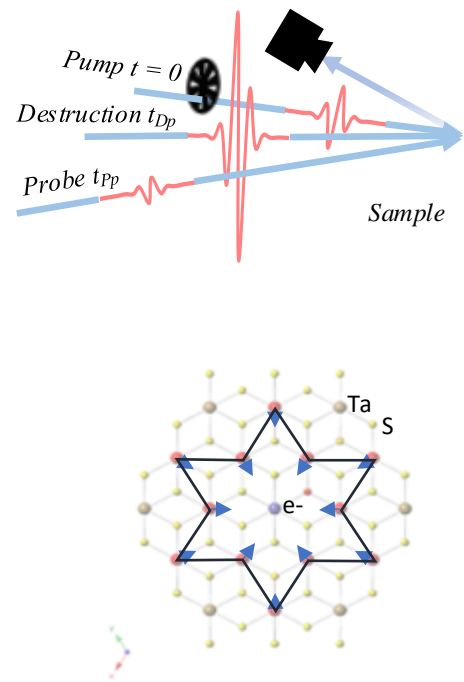


L. Stojchevska,^{1,2} I. Vaskivskiy,¹ T. Mertelj,¹ P. Kusar,¹ D. Svetin,¹ S. Brazovskii,^{3,4} D. Mihailovic^{1,2,5*}



Collective mode frequency switching in 1T-TaS₂

Resistance switching to a 'hidden' state

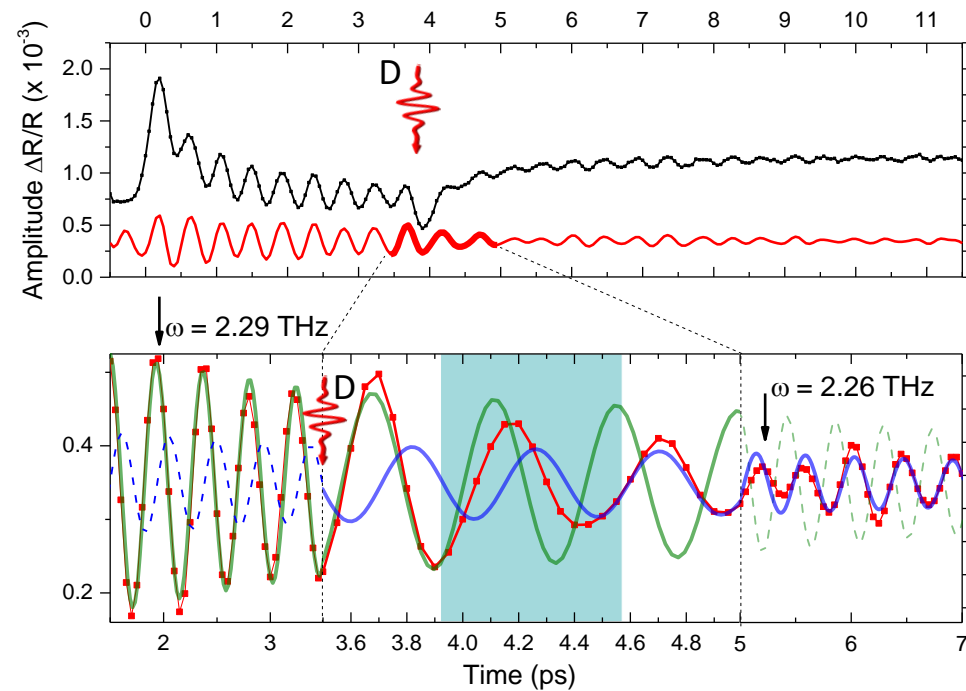
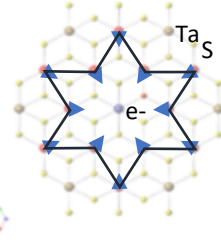


Demsar et al, Phys. Rev B (2002); Demsar et al, Phys. Rev. Lett (1999); Stojchevska et al. Science (2014)

Coherent switching control

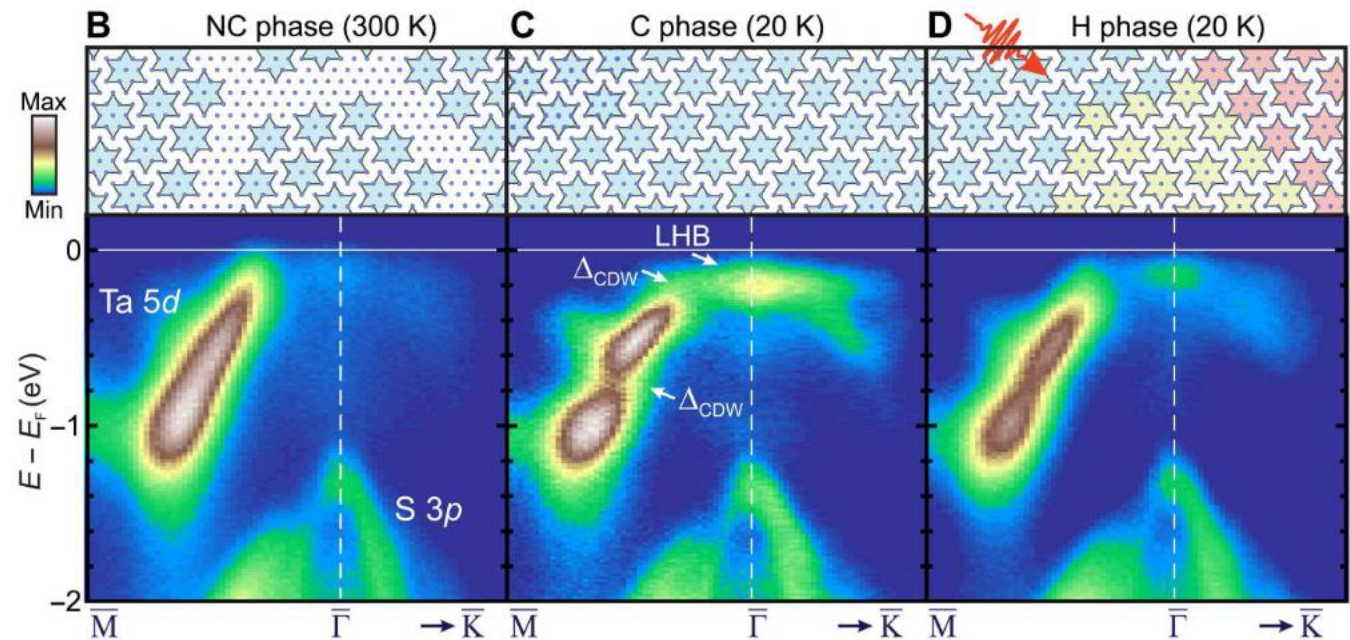
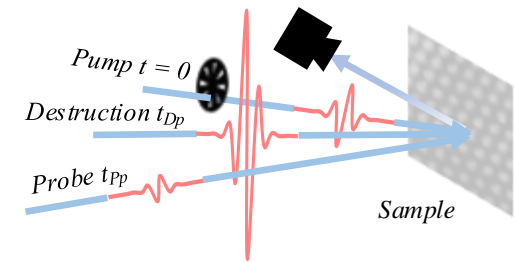
Multipulse optical coherent control

Ravnik, et al., *Phys Rev B* **97**, e1400173 (2018).



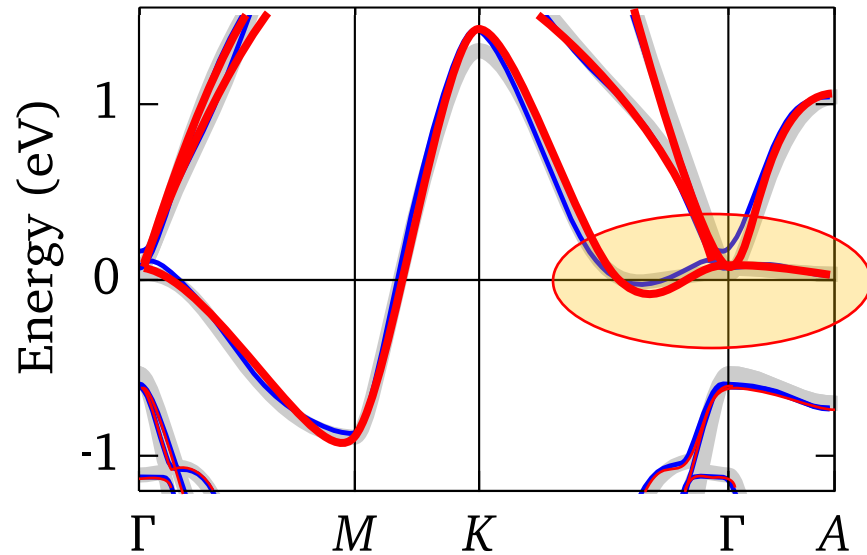
Multipulse ARPES coherent control

Maklar et al, *Science advances* **9**, eadi4661 (2023)



The C-H transition takes place in < 400 fs.

Undistorted 1T-TaS₂ exhibits a flat band at E_F along $\Gamma - K$.



Carriers are prone to localisation
(formation of polarons):

The threshold for localization is defined by
the dimensionless parameter, the Wigner-
Seitz radius $r_s = \frac{a}{a_{Bohr}}$

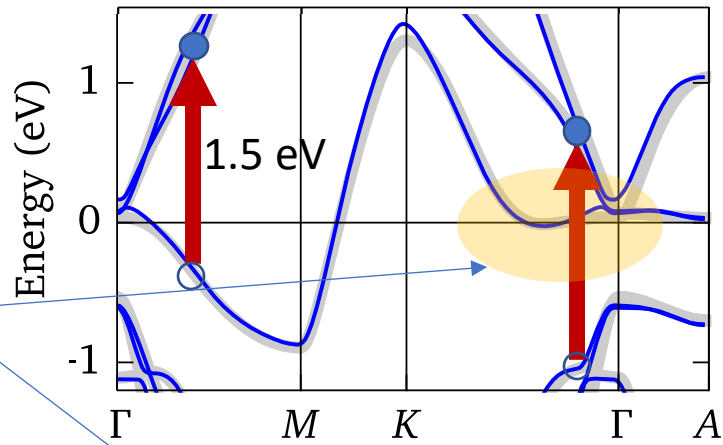
$$r_s = \frac{a}{a_{Bohr}}$$

$$\text{In 2D, } r_s = \frac{V}{t} = \frac{e^2 m^*}{\hbar^2 \sqrt{n}} = 31 \sim 38^\dagger$$

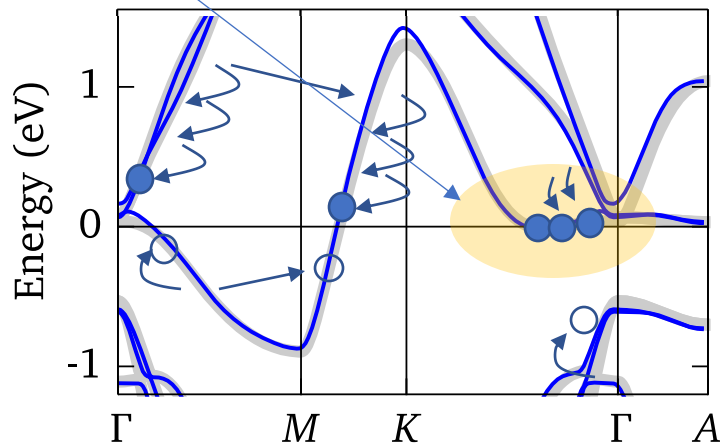
$$1\text{T-TaS}_2: f=1/13, m^* \sim 3 - 5m_e \rightarrow r_s = \frac{V}{t} = 70 \sim 100$$

Photodoping in 1T-TaS₂ : carrier localization and jamming

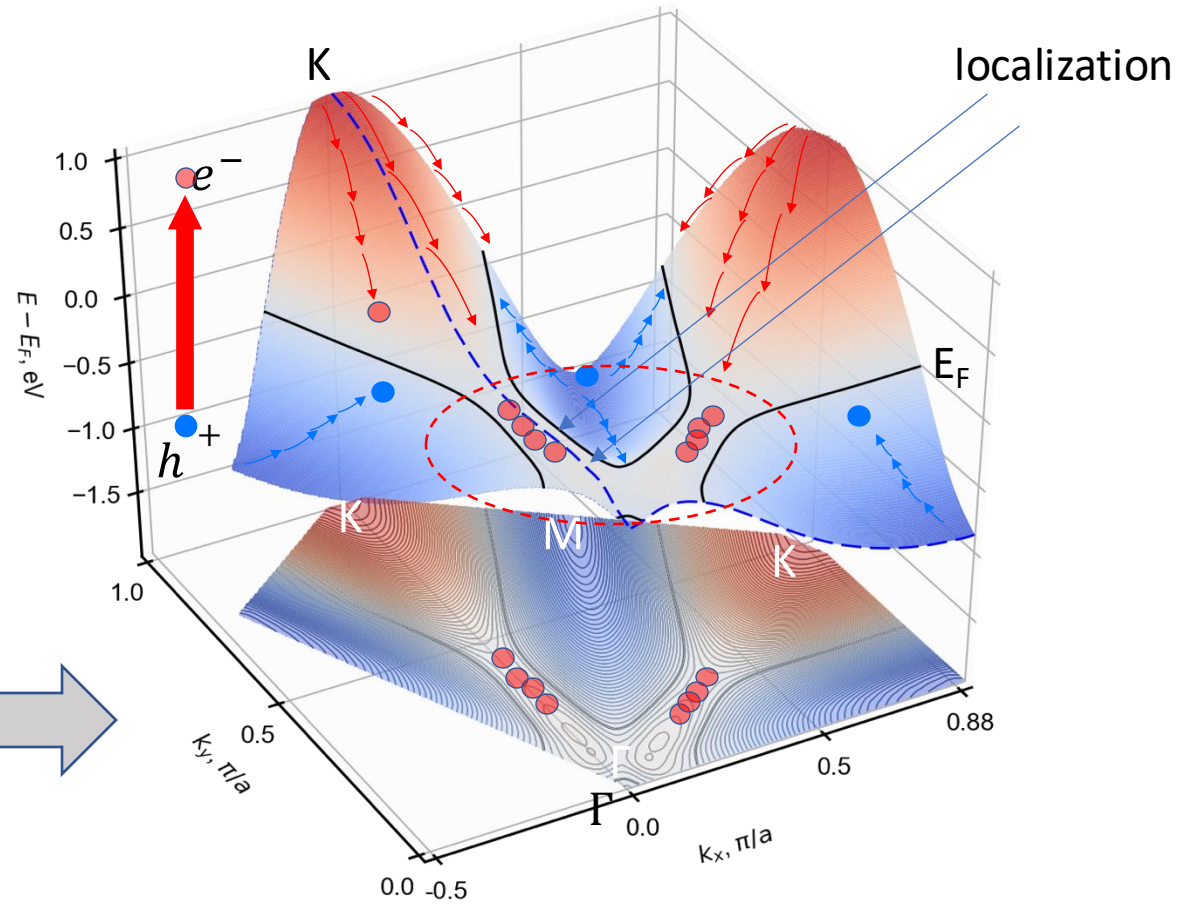
Band structure has a single Ta band within +/-1 eV, with a flat band near the Γ point.



e^- and h^+ thermalization via phonons shows an imbalance, leading to electron condensation



1T-TaS₂ band structure from Ritschel, Nat. Phys. 2014

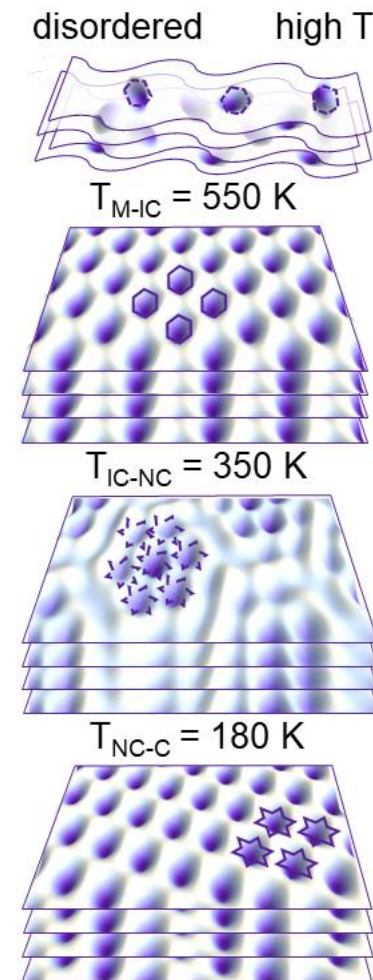
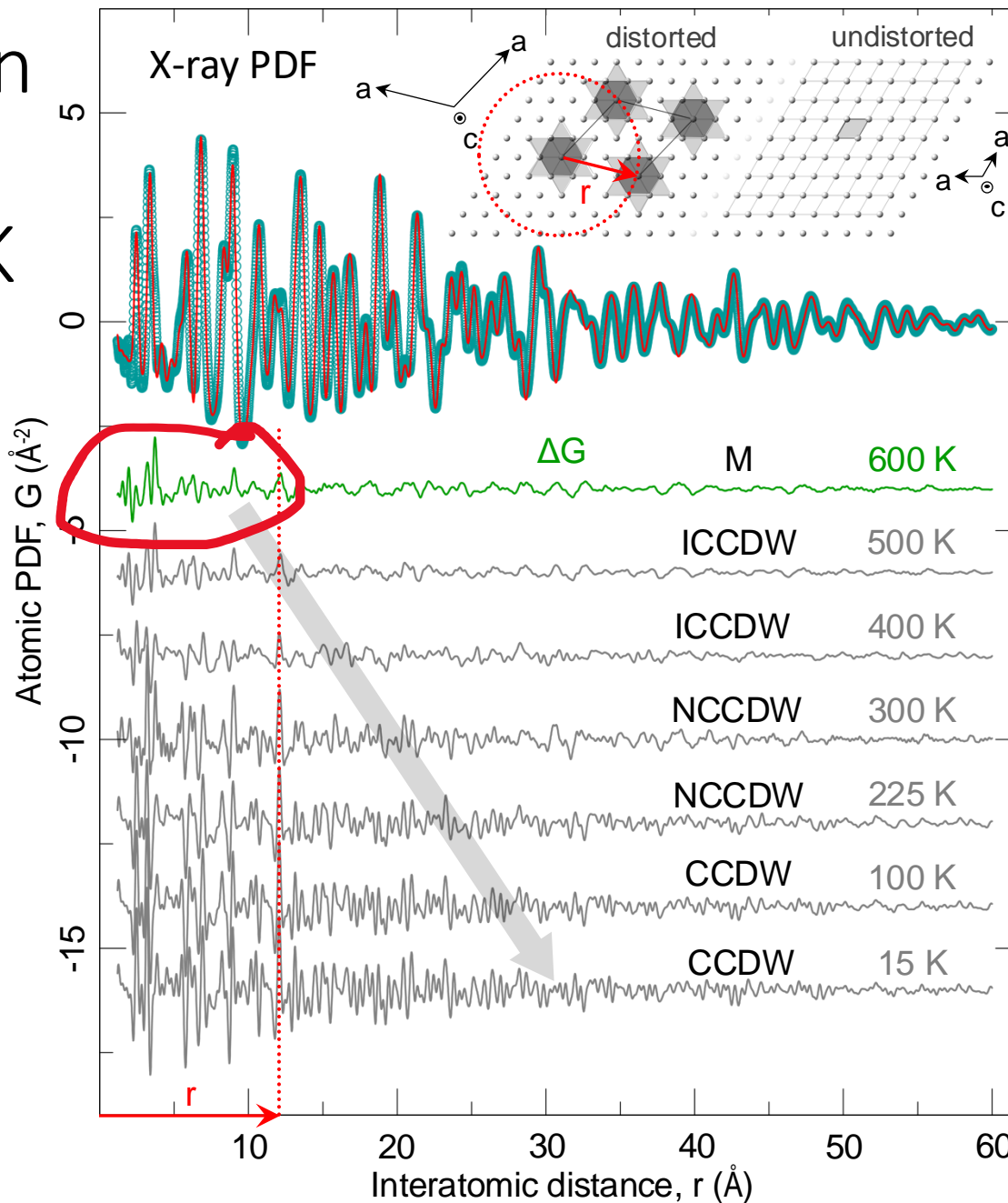
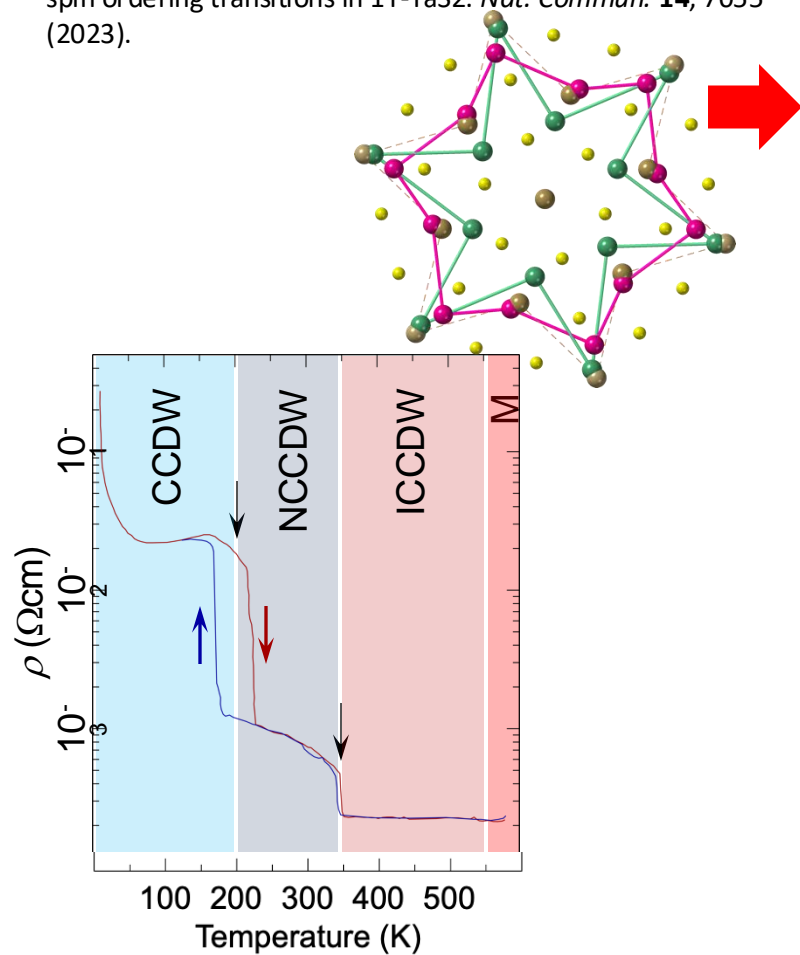


Polaron signatures in the local structure from 15 K to > 600 K

Bozin, E. S. *et al.* Crystallization of polarons through charge and spin ordering transitions in 1T-TaS₂. *Nat. Commun.* **14**, 7055 (2023).



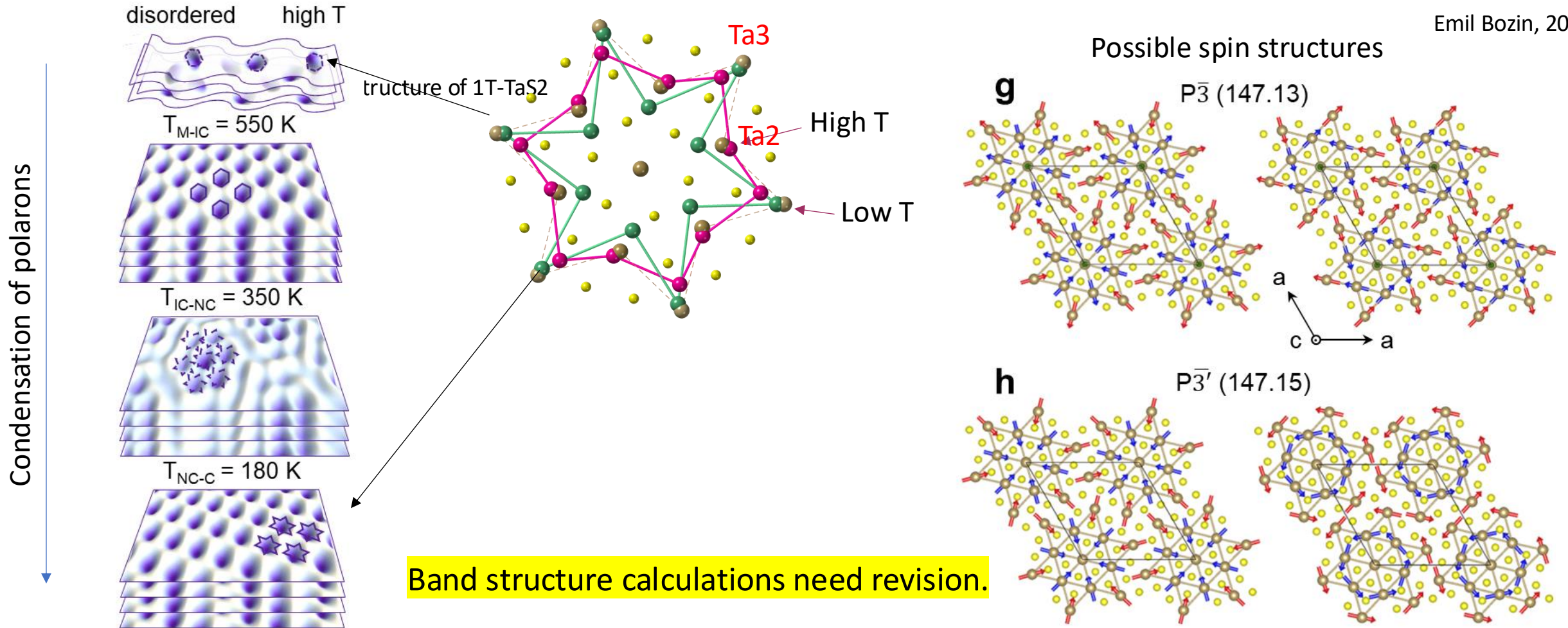
Emil Bozin,



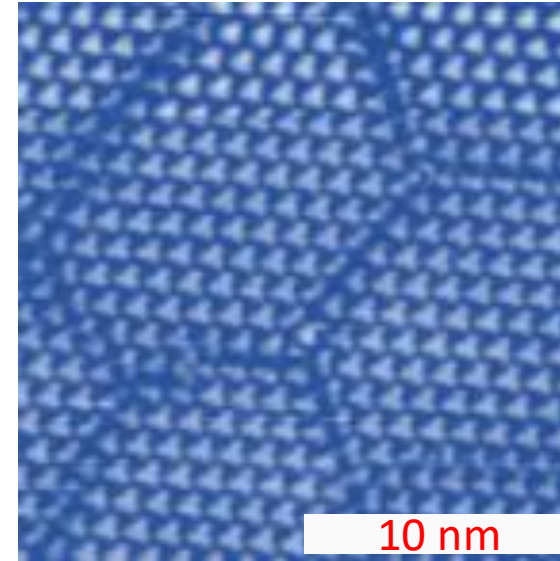
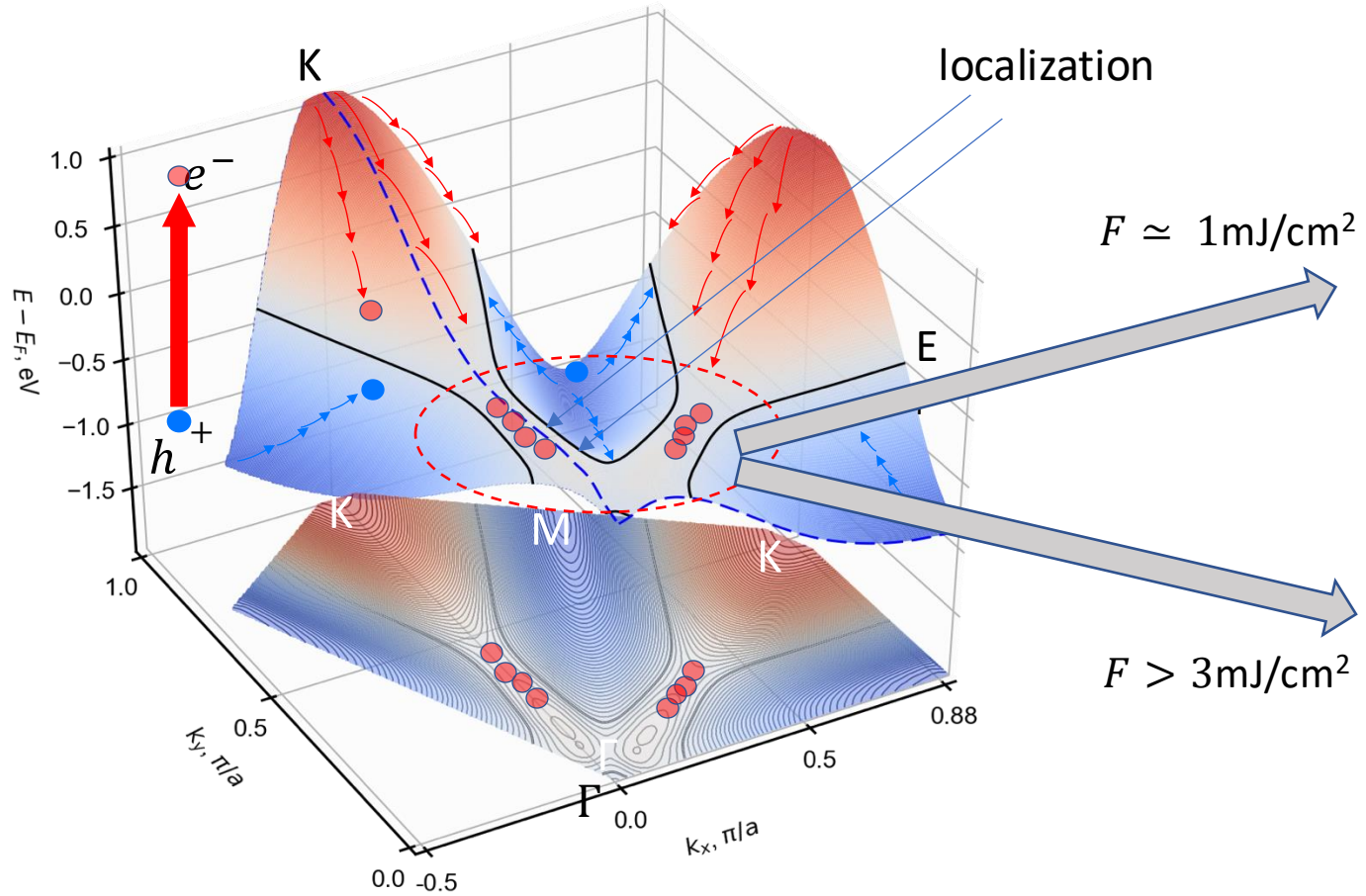
Symmetry-breaking polaron fluctuations at high temperature (X-ray PDF) and a sequence of orders on reducing T



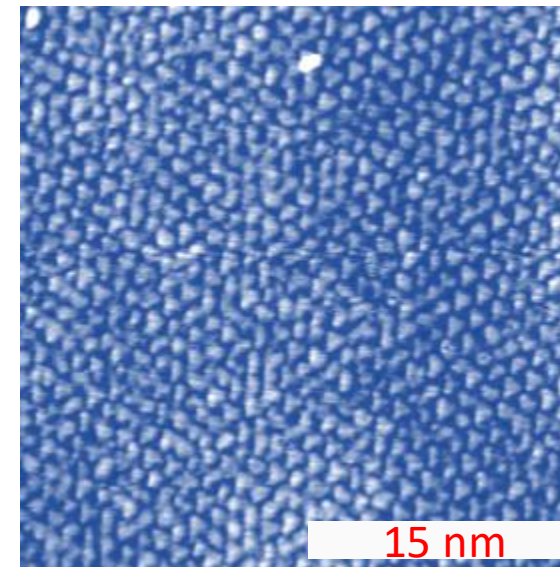
Emil Bozin, 2022



Different hidden states reached by varying the excitation conditions

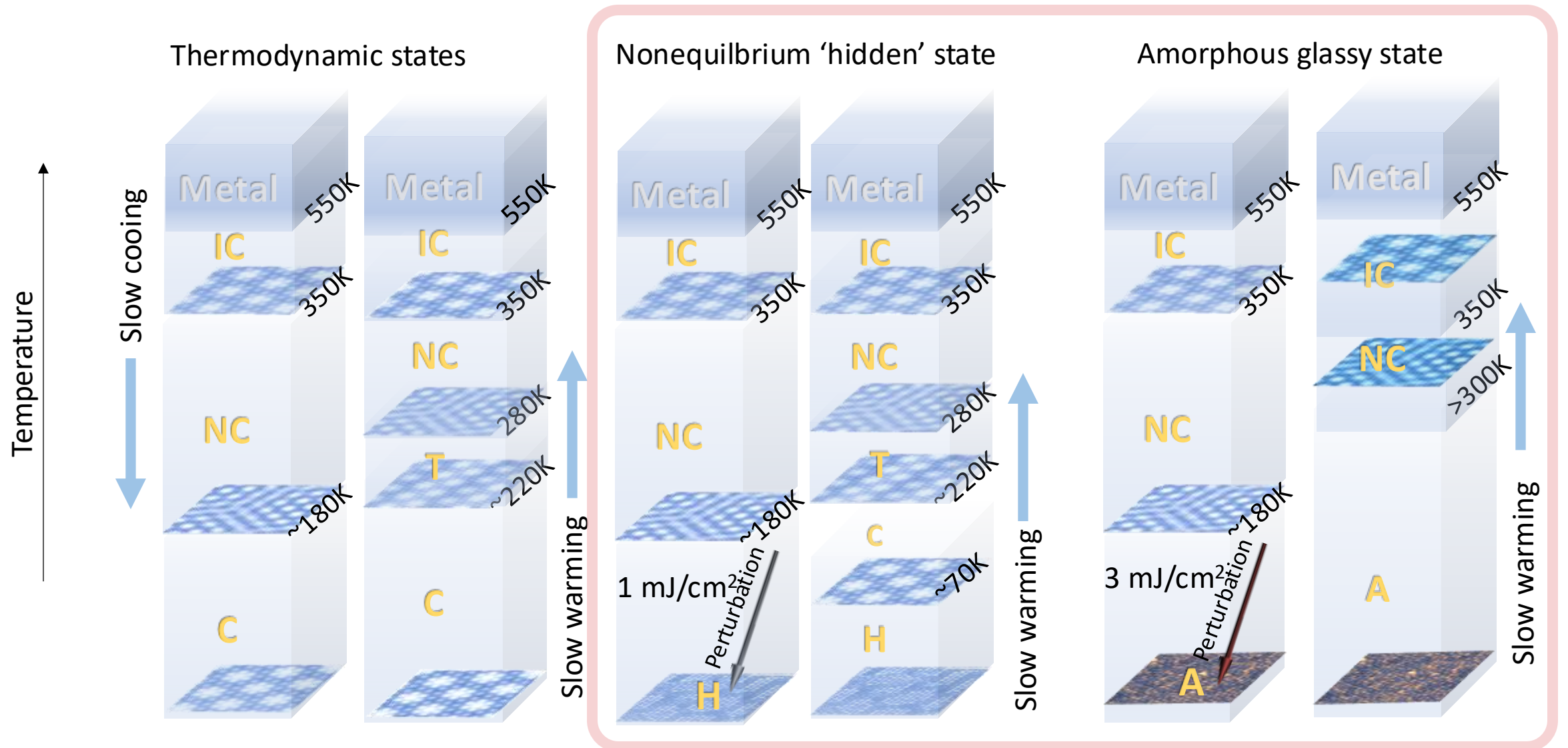


'Hidden domain state'
Stojchevska et al *Science* 2014

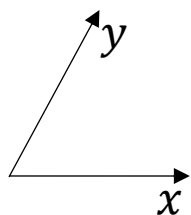
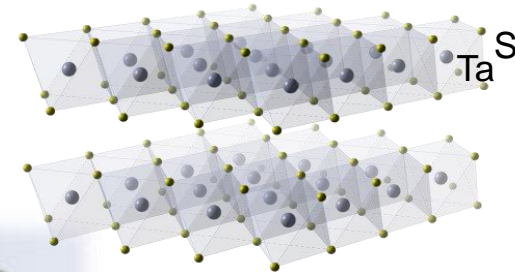


Amorphous
electronic state
Gerasimenko et al *Nat Mat* 2019

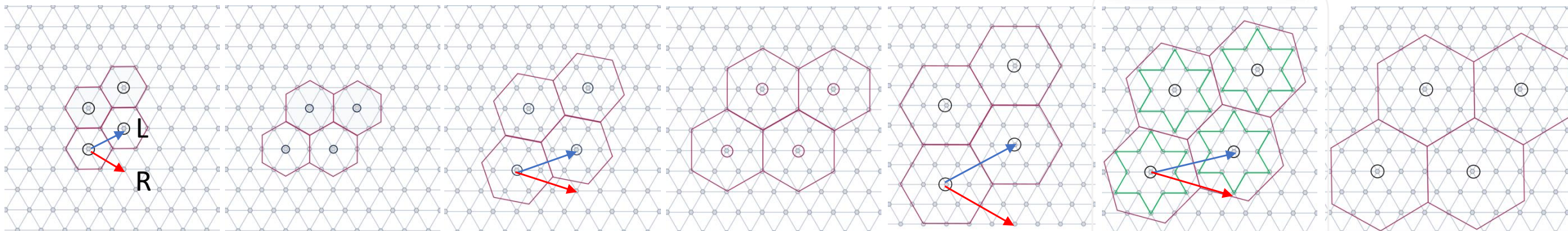
Metastable and thermodynamic phases of 1T-TaS₂



Magic superlattices and Wigner crystals



$$\frac{1}{f} = x^2 + y^2 + xy, \text{ where } x, y \text{ are integers}$$



$$\frac{1}{f} = 3$$

$(x = 1, y = 1)$

$$\frac{1}{f} = 4$$

$(x = 2, y = 0)$

$$\frac{1}{f} = 7$$

$(x = 2, y = 1)$

$$\frac{1}{f} = 9$$

$(x = 3, y = 0)$

$$\frac{1}{f} = 12$$

$(x = 2, y = 2)$

$$\frac{1}{f} = 13$$

$(x = 3, y = 1)$

$$\frac{1}{f} = 16$$

$(x = 4, y = 0)$

2H-Fe_{0.33}TaS₂

1T-TiSe₂,
2H-Fe_{0.33}TaSe₂,
2H-Fe_{0.33}NbSe₂,
1T-Cu_{0.08}TiSe₂

2H-TaS₂
2H-TaSe₂

H-1T-TaS₂
1T-Ti_{0.07}Ta_{0.93}Se₂,
1T-TaSeS
1T-Ta_{0.99}Fe_{0.01}S₂

1T-TaS₂,
1T-Ti_{0.07}Ta_{0.93}Se₂,
1T-TaSeS
1T-Ta_{0.99}Fe_{0.01}S₂

1T-VSe₂

Modelling of Wigner crystal superlattices



Jaka Vodeb

Classical charged lattice gas model with screened coulomb interaction:

$$\mathcal{H} = \sum_{i < j} V(i, j) n_i n_j,$$

where

$$V(i, j) = V_0 \frac{\exp(-r_{ij}/r_s)}{r_{ij}}$$

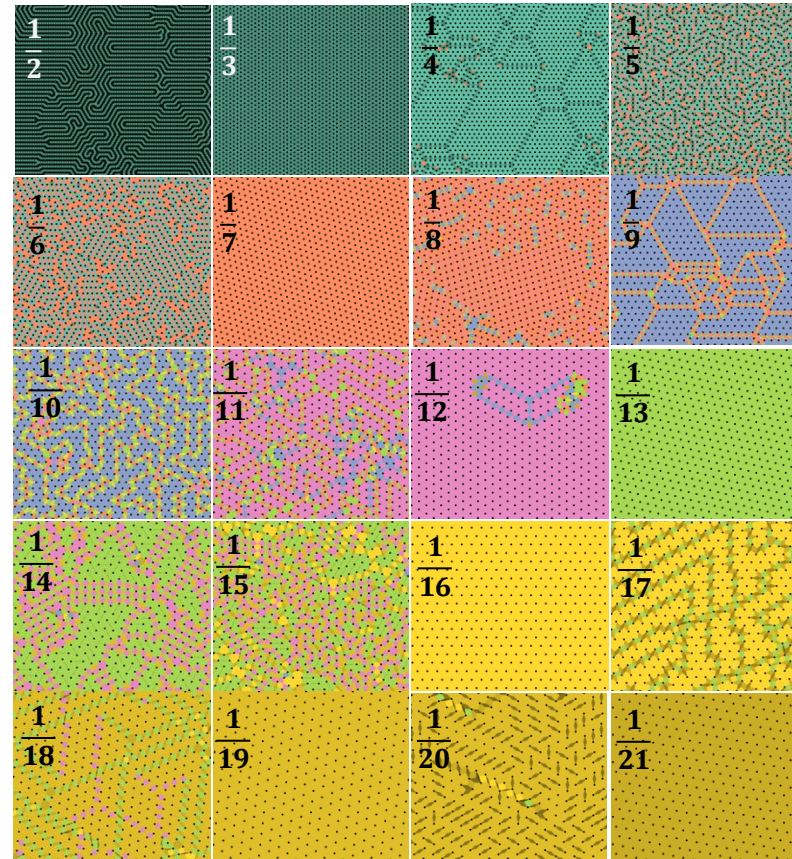
Valid when $r_s = \frac{V}{T} \gg 1$

T is the kinetic energy

Commensurate structures satisfy:

$$\frac{1}{f} = x^2 + y^2 + xy,$$

where x and y are integers

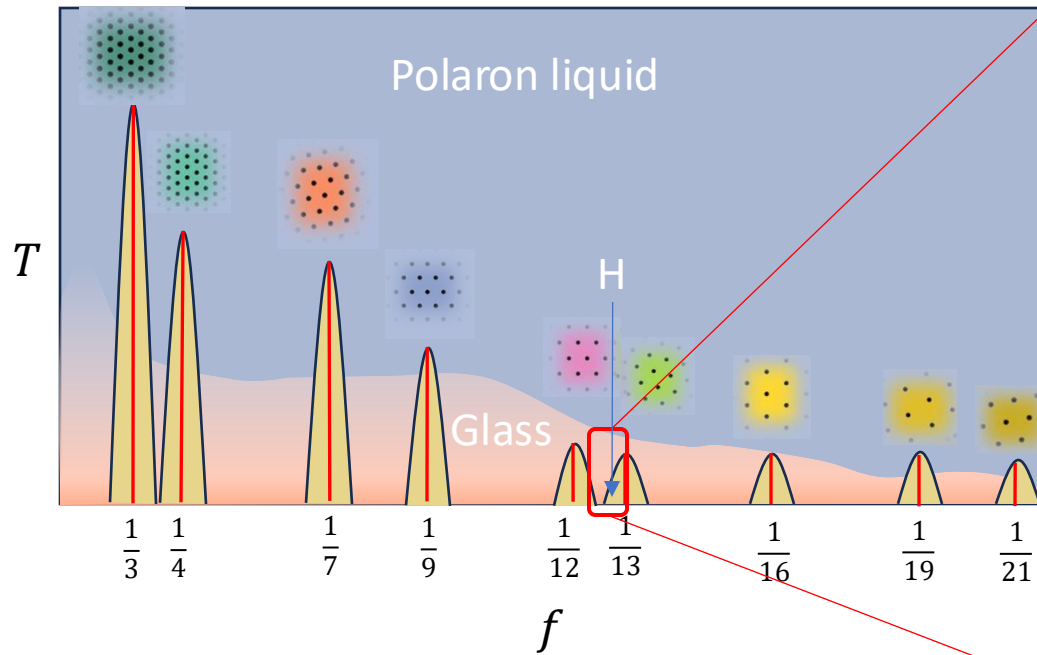


System	f	Phase
2H-Fe _{0.33} TaS ₂	1/3	crystal
1T-TiSe ₂	1/4	crystal
1T-Cu _{0.08} TiSe ₂	1/4.2	domain state
2H-Fe _{0.33} TaSe ₂	1/4	crystal
2H-Fe _{0.33} NbSe ₂	1/4	crystal
2H-TaS ₂	1/9	crystal
2H-TaSe ₂	1/9	crystal
2H-NbSe ₂	~ 1/9	domain state
1T-TaS ₂	1/13	crystal
PD 1T-TaS ₂	1/12.6	domain state
1T-TaSeS	1/12.6	domain state
1T-Ta _{0.99} Fe _{0.01} S ₂	1/12.6	domain state
1T-Nb _{0.04} TaS ₂	~ 1/13	domain state
1T-Nb _{0.07} TaS ₂	~ 1/13	domain state
PD 1T-TaS ₂	1/11	amorphous state
1T-Nb _{0.1} TaS ₂	~ 1/11	possible amorphous state
4Hb-TaS ₂	1/13	crystal
1T-TaSe ₂	1/13	crystal
1T-Ti _{0.07} Ta _{0.93} Se ₂	1/12.6	domain state
4Hb-TaSe ₂	1/13	crystal
1T-NbSe ₂	1/13	crystal
1T-VSe ₂	1/16	crystal

Karpov, P. & Brazovskii, S. *Sci Rep* **8**, 1–7 (2018).

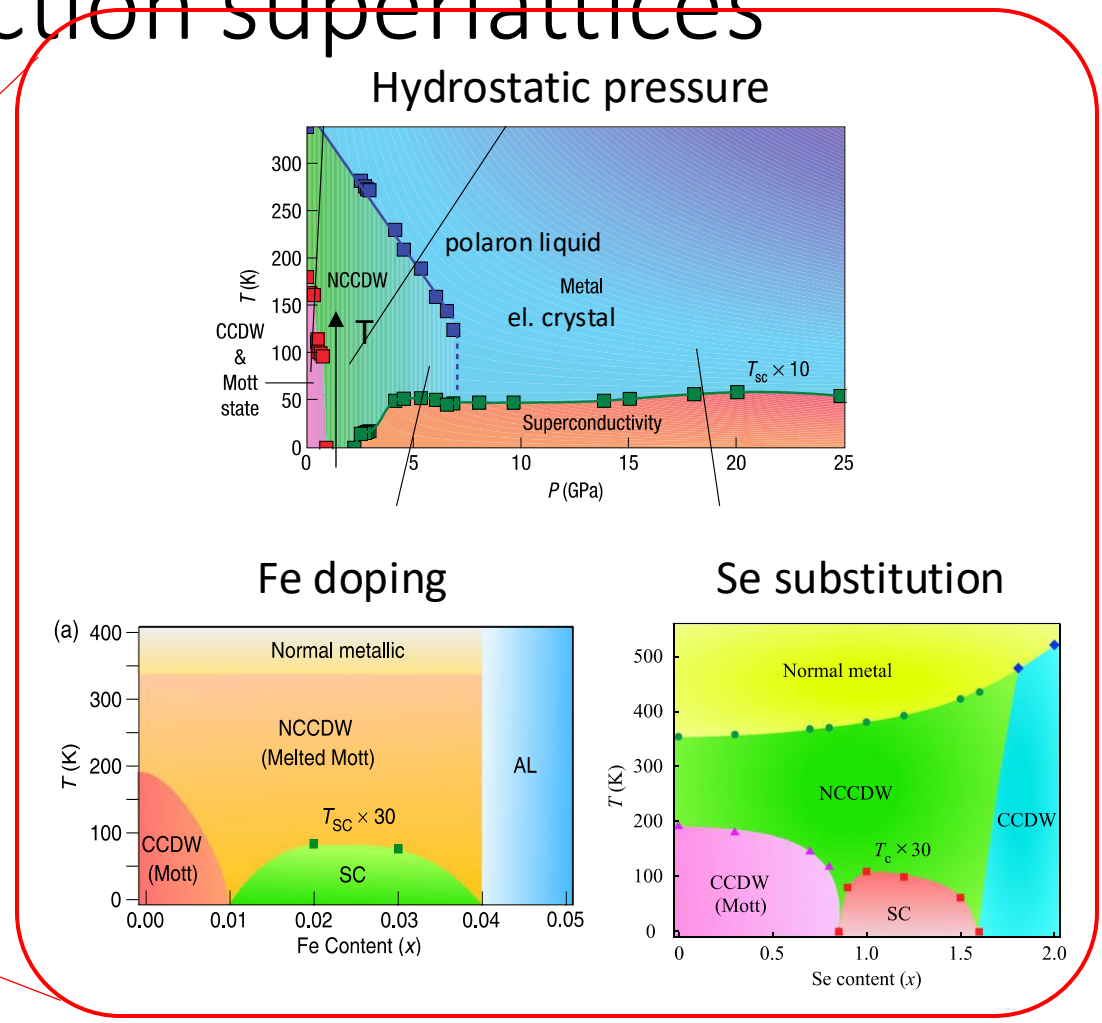
Vodeb, J. *et al. New J Phys* **21**, 083001 (2019).

Phase diagram of magical fraction superlattices

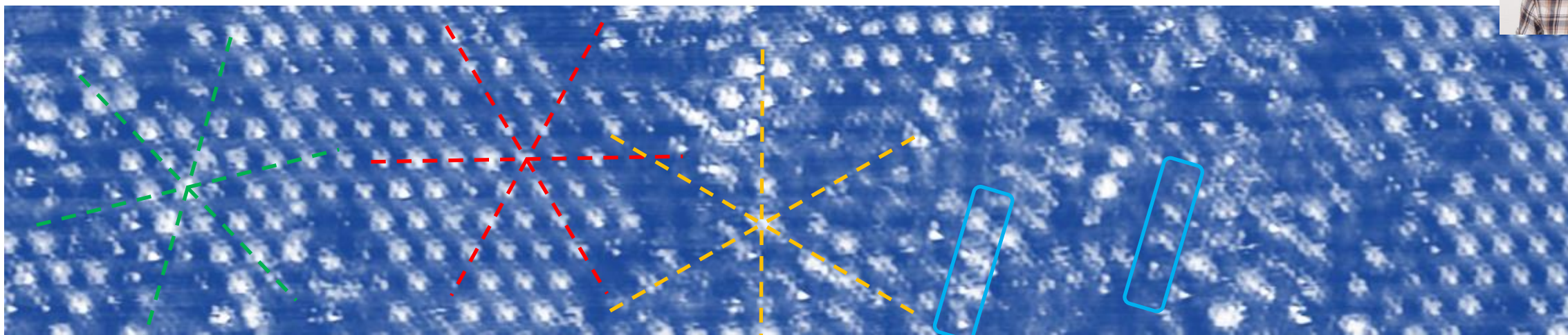
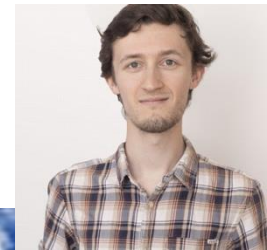


NB: WC physics is dominant for small t and large $r_s = V/t$

t is determined by the e-p coupling strength of conduction band electrons



Coexisting metastable superlattices after photoexcitation

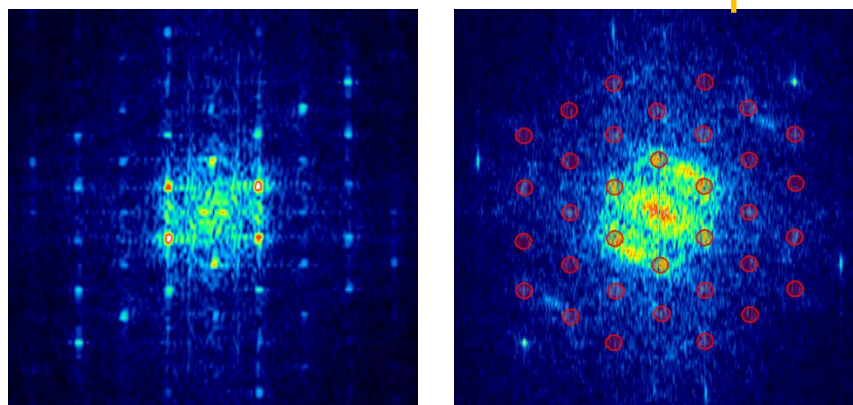


Crystal lattice

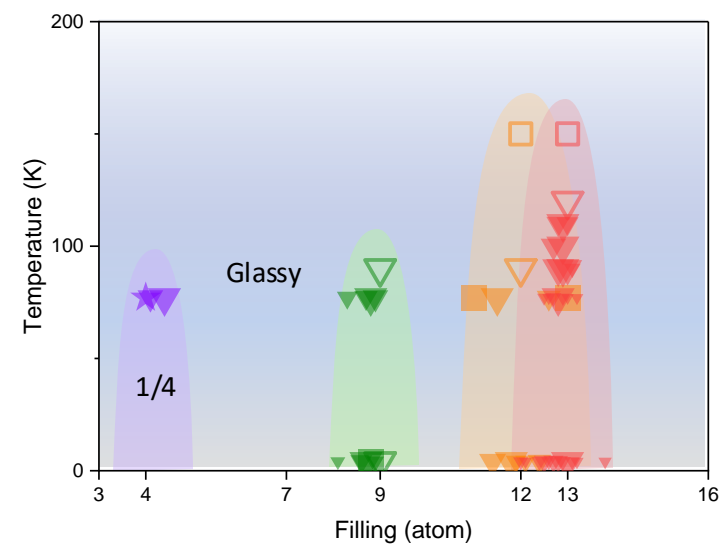
$1/13 L$

$1/13 R$

$1/9$

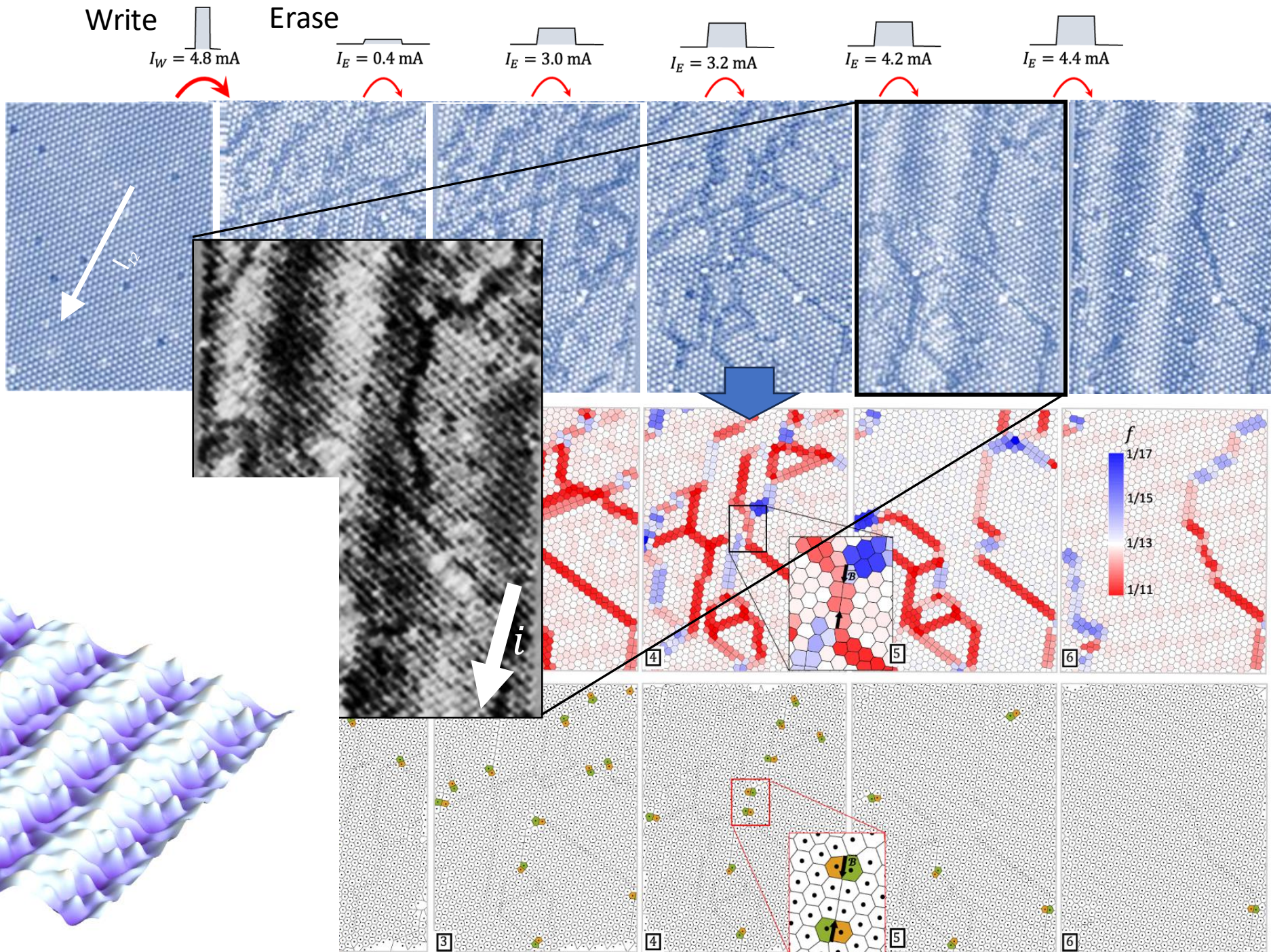
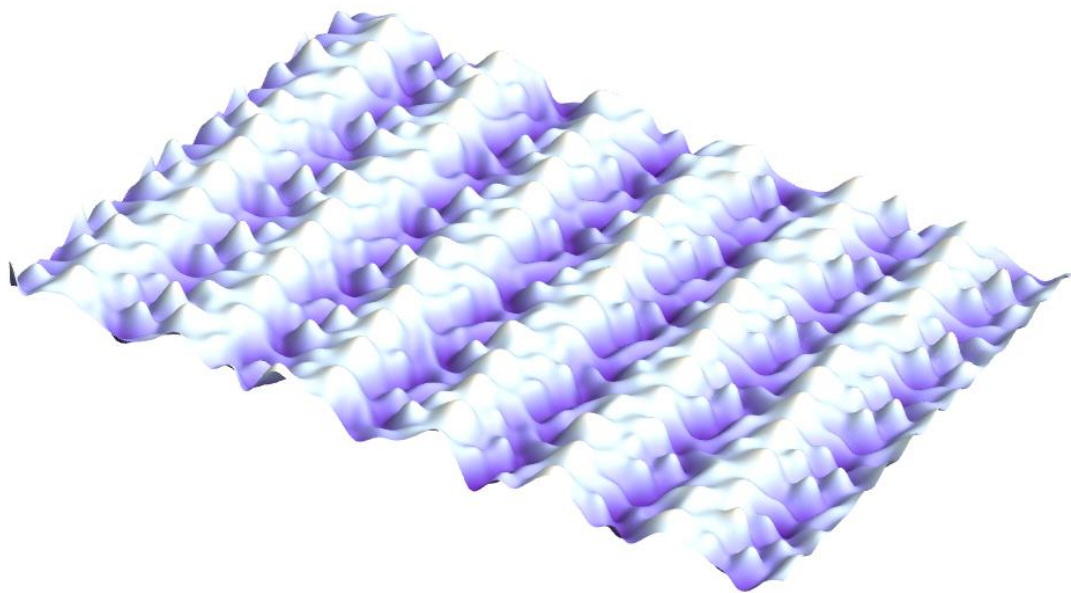


4 K



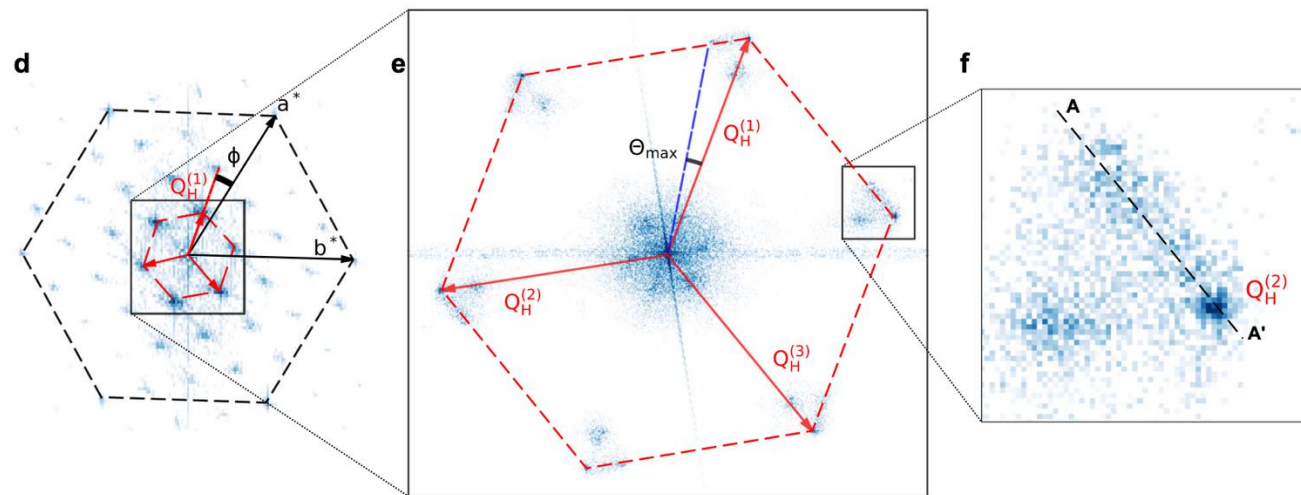
STM experiment: Wigner-Seitz tessellation and non-trivial defects

Raw STM images

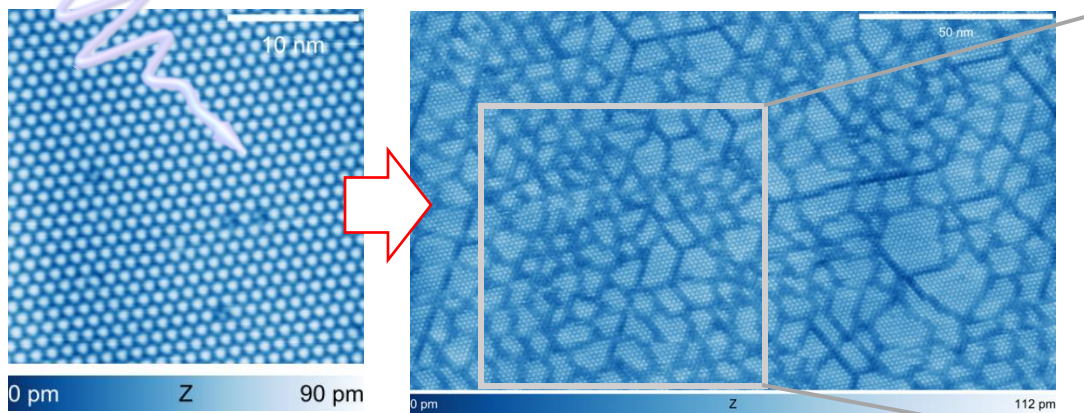


The hidden state shows emergent mesoscopic orders

Gerasimenko et al., npj Quantum Materials, **4**, 32 (2019)

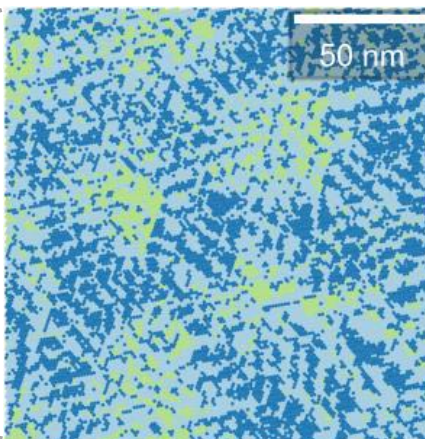


STM topography



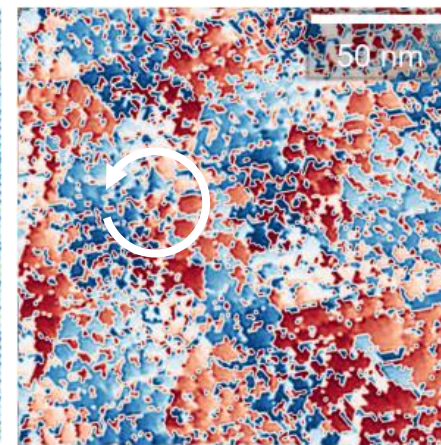
35 fs, 1 mJ/cm²
laser pulse, or
electrical pulse

Displacement
 $|\vec{D}|$



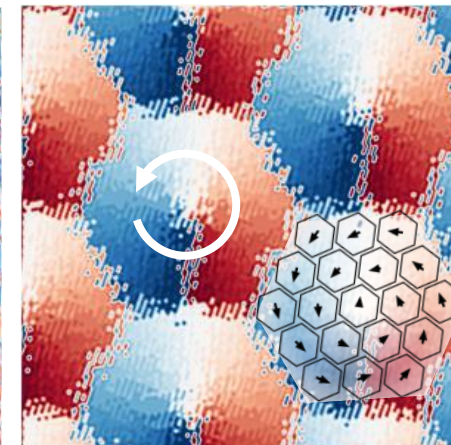
0 a a√3
 \vec{D} , atomic units

Displacement angle
 α



-180 0 180
Direction α , deg.

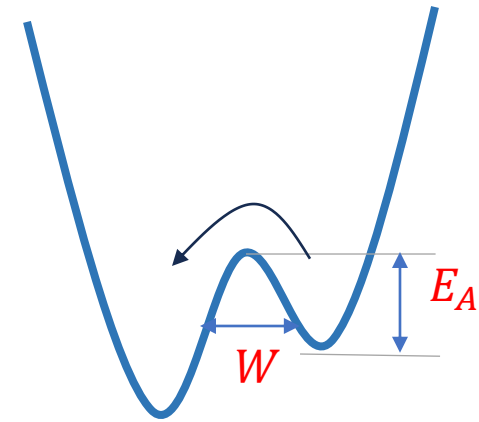
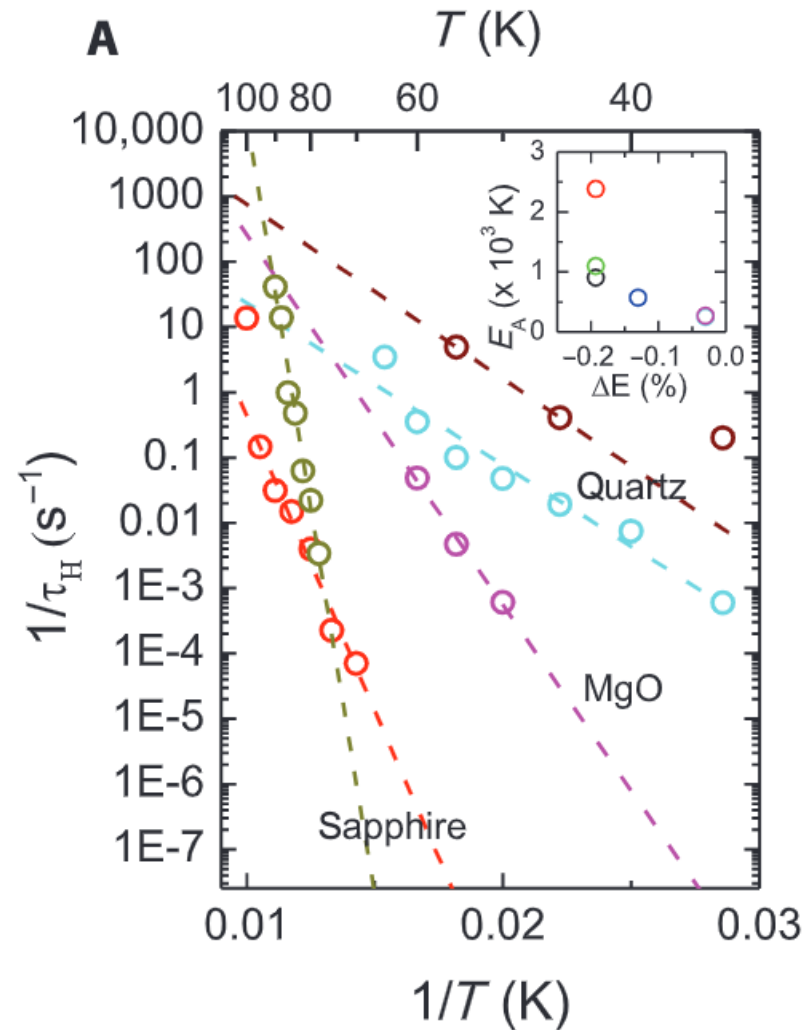
Simulation of α



\vec{D}

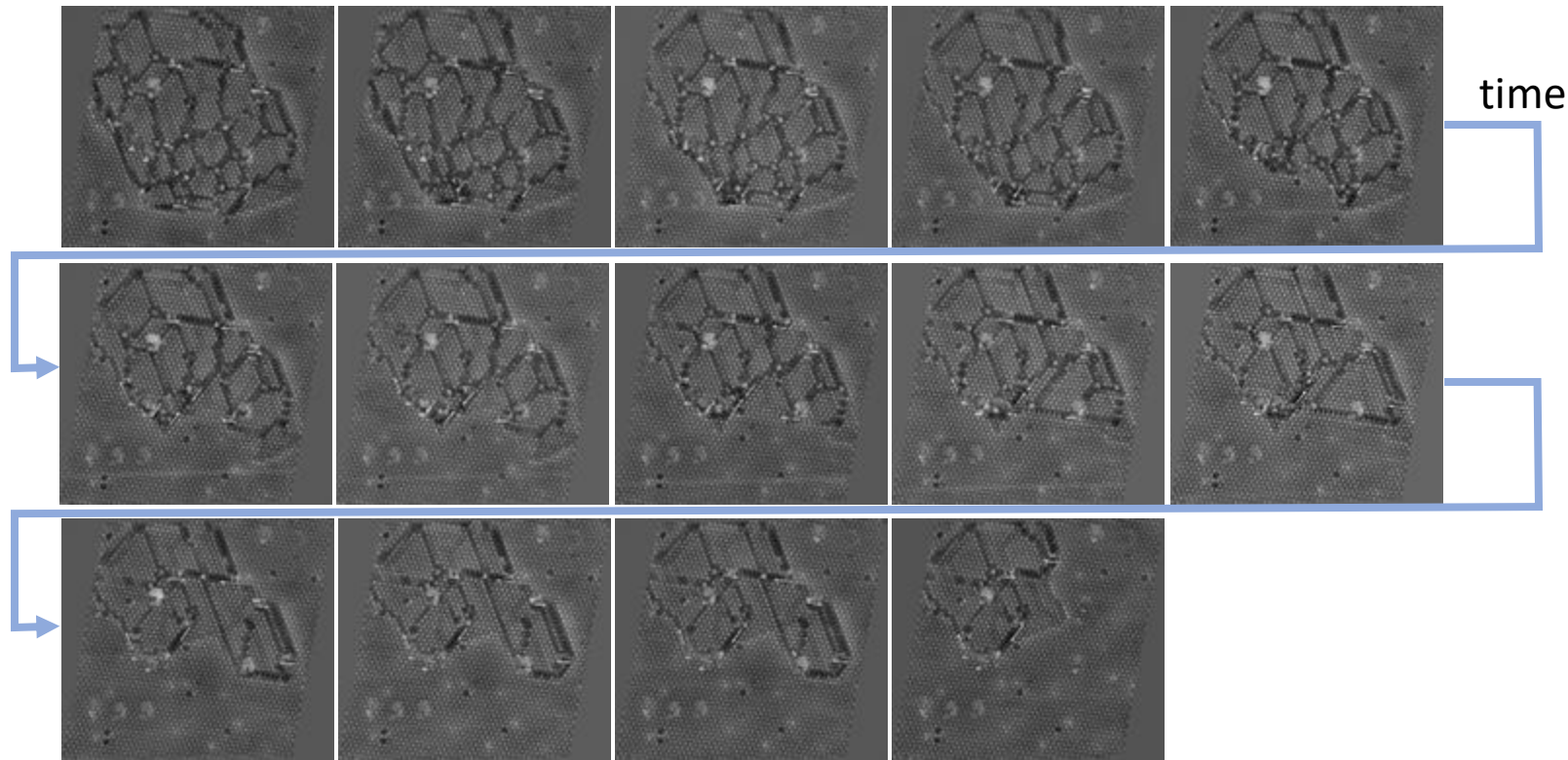
Dynamics

The Hidden state relaxation time depends on temperature and strain

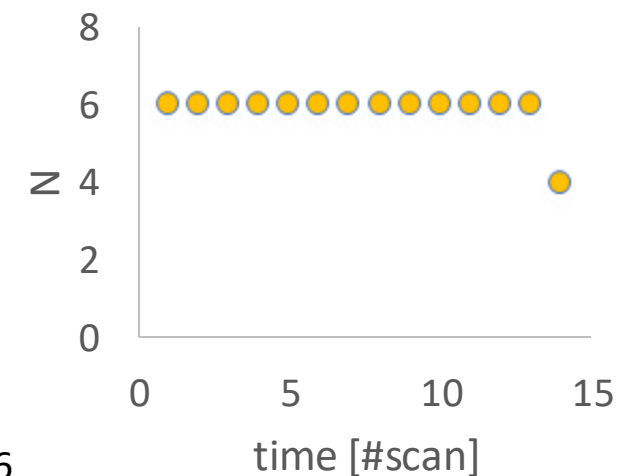
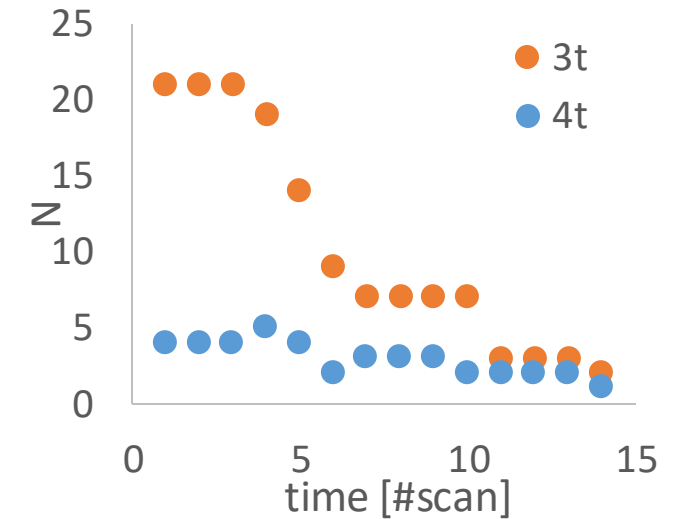


Vaskivskiy, I. *et al.* Controlling the metal-to-insulator relaxation of the metastable hidden quantum state in 1T-TaS₂. *Sci Adv* **1**, e1500168 (2015).

Spontaneous relaxation through configurational states

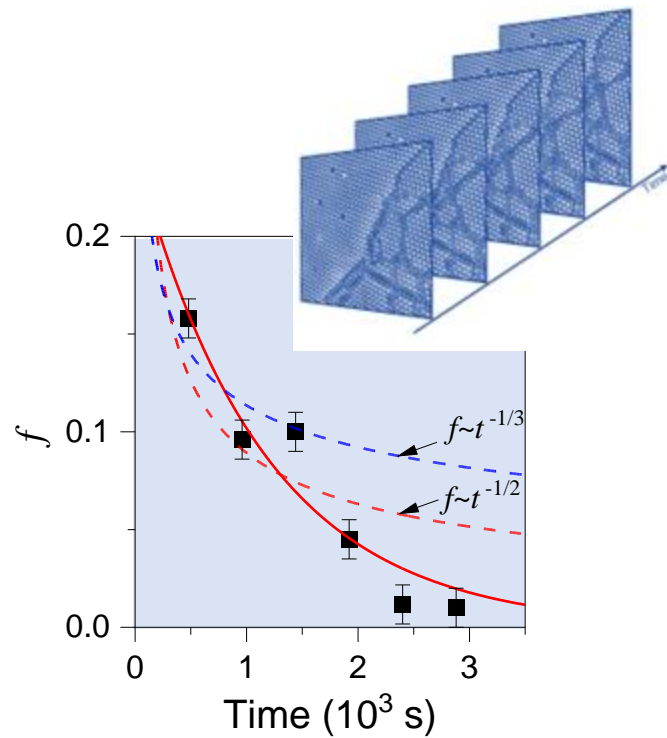


Topologically non-trivial defects stabilize the 'hidden' domain state

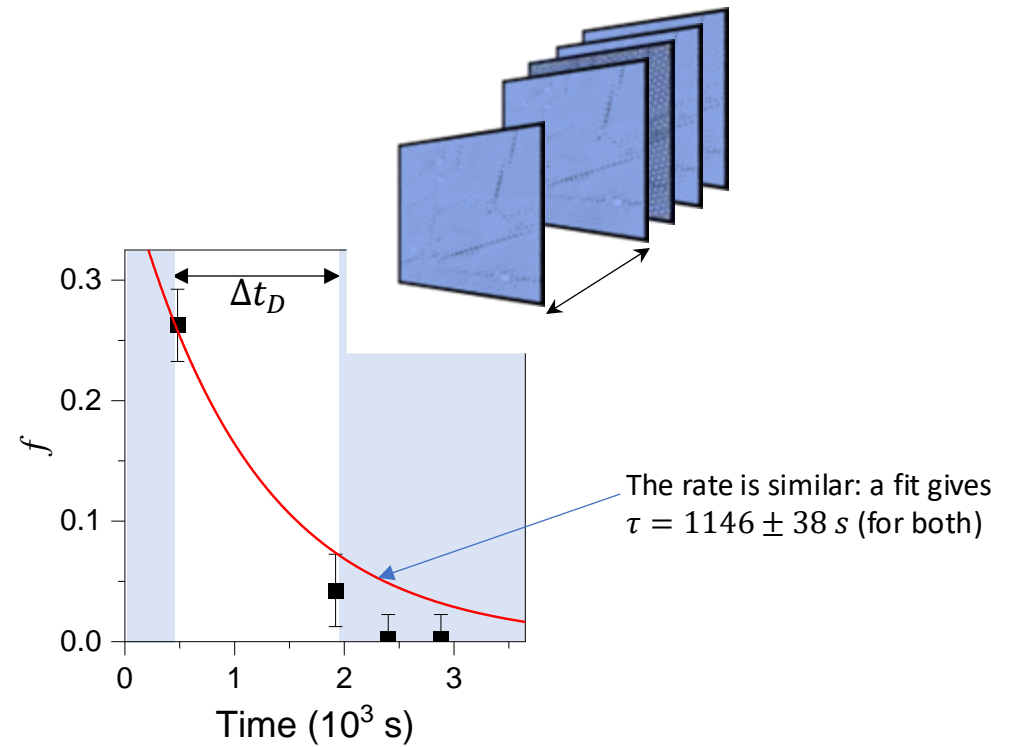


Tip-enhanced relaxation?

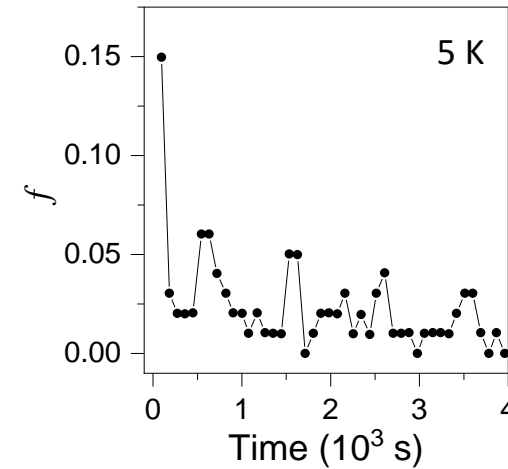
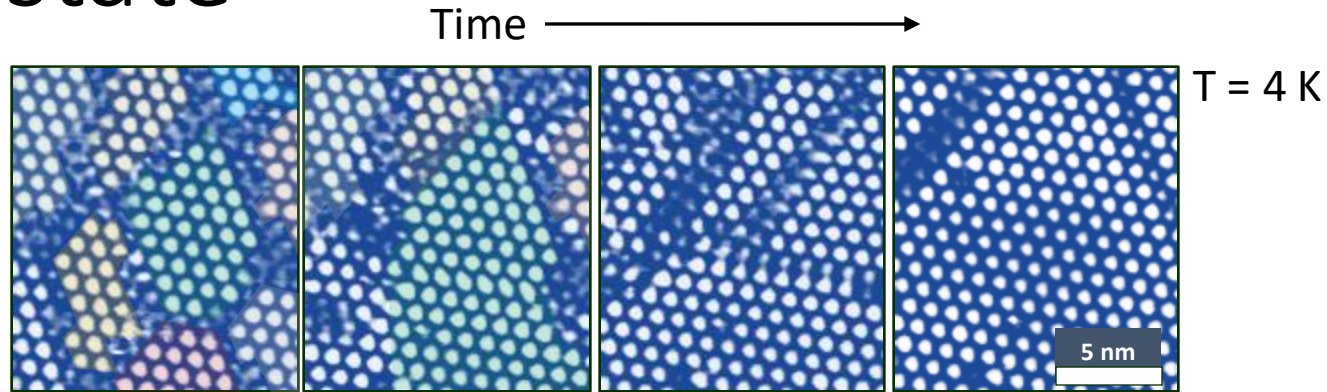
Relaxation **with** tip scanning



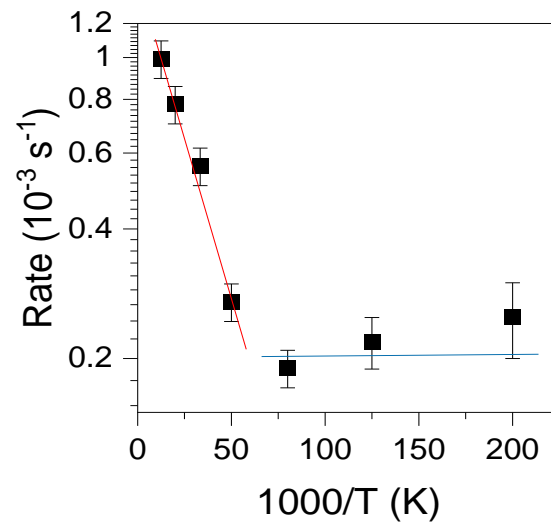
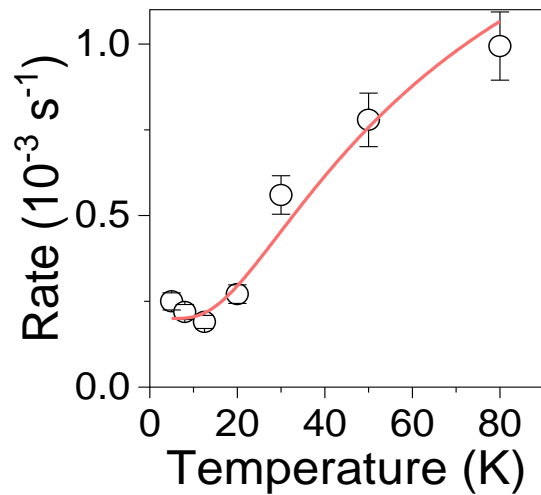
Relaxation with **NO** tip scanning



Spontaneous decay dynamics of the domain state



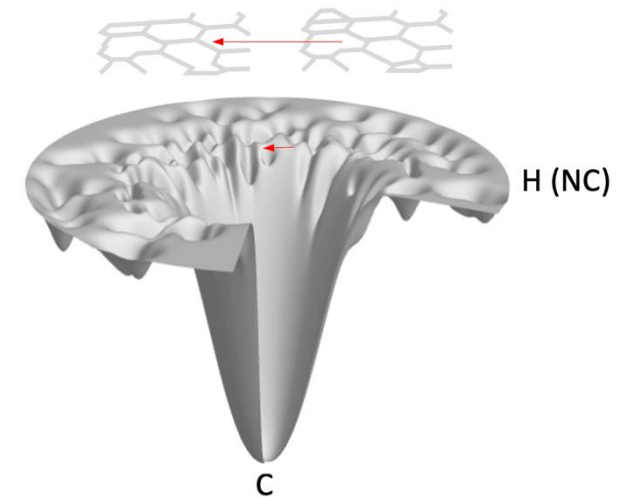
f = 'Hamming distance' (how many polarons have moved from one configuration to another)



$$R(T) = R_q + R_0 e^{-E_B/k_B T}$$

E_B is determined by the energy difference between configurational states

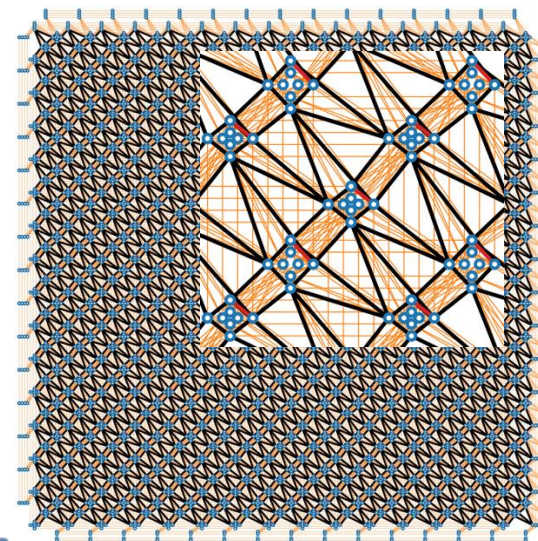
R_0 is related to the Hamming distance



Quantum simulations

From CLG via Jordan-Wigner transformation:

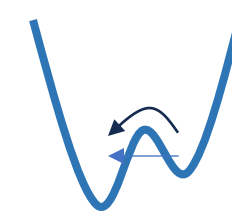
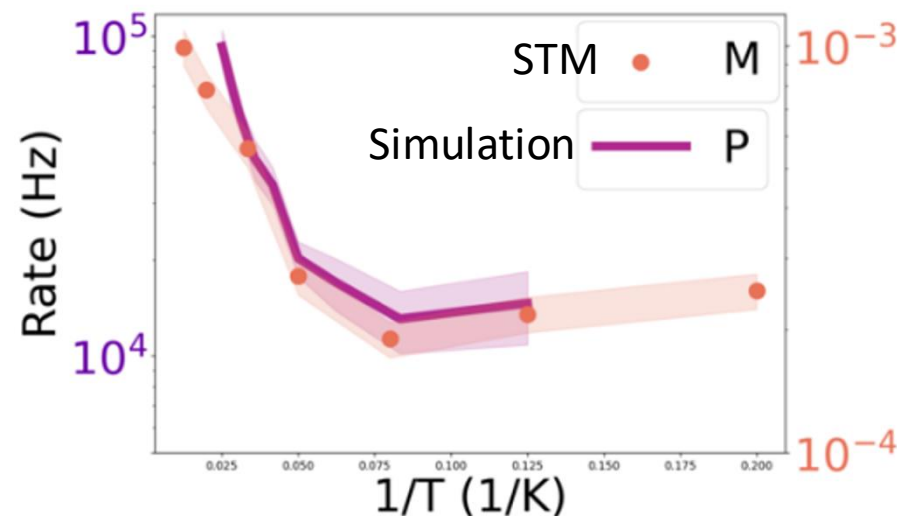
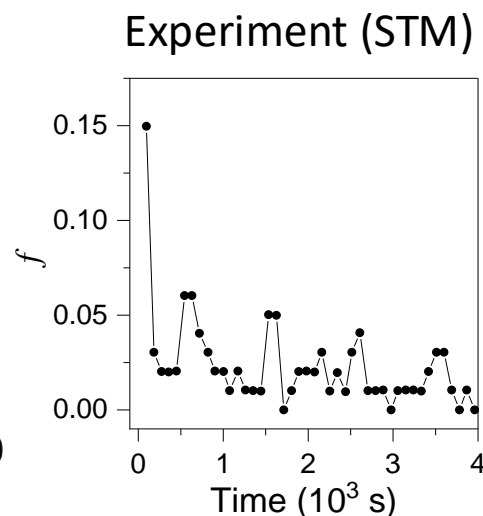
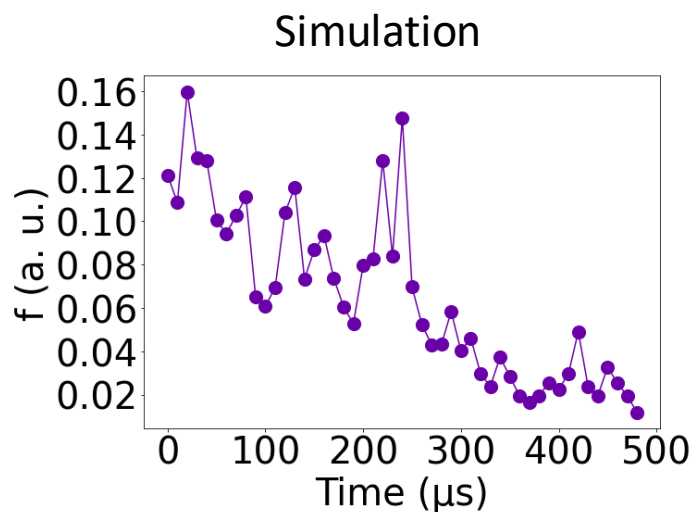
$$H_S = -A(s) \sum_i \sigma_i^x / 2 + B(s) \left(\sum_{i<j} J_{i,j} \sigma_i^z \sigma_j^z + \sum_i h_i \sigma_i^z \right) / 2$$



Custom embedding
on the D-wave
Advantage 6.1 QPU

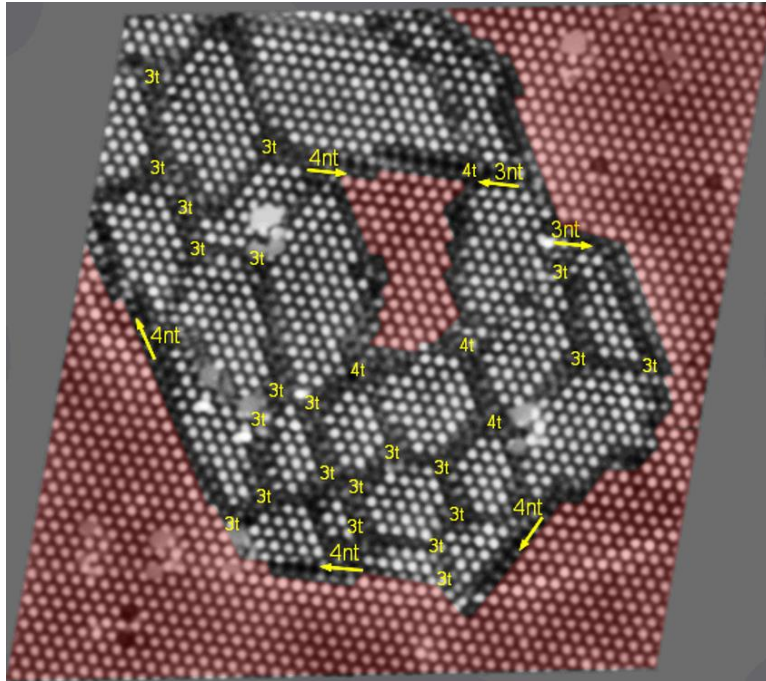


Vodeb et al., Nat. Comm. 15, 4836 (2024).

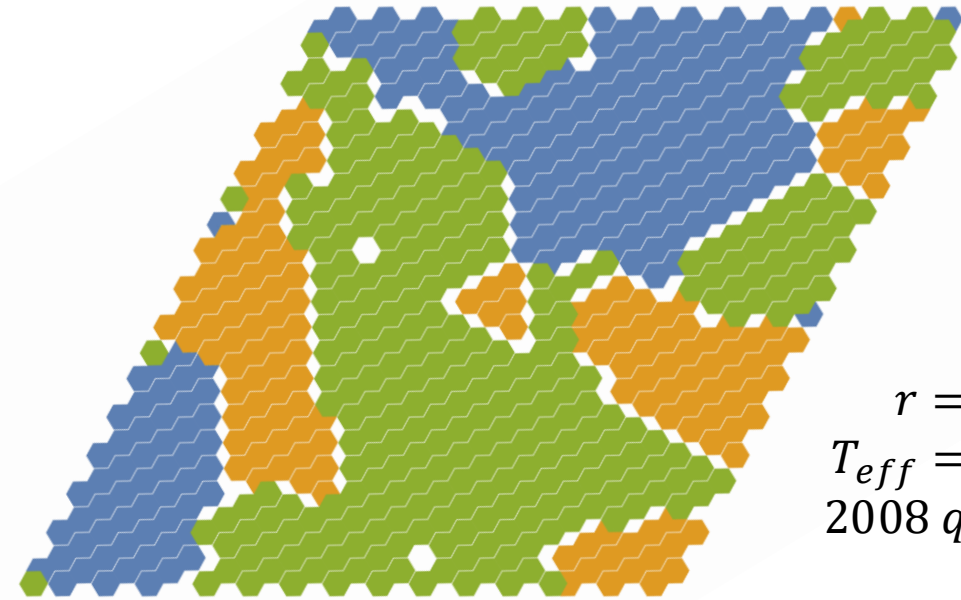


Experiment and simulation of quantum decay

Sequence of STM images
~30 minutes per image



STM topography:
Domain state decay at 4 K in 1T-TaS₂



$r = 9$
 $T_{eff} = 1.33$
2008 qubits

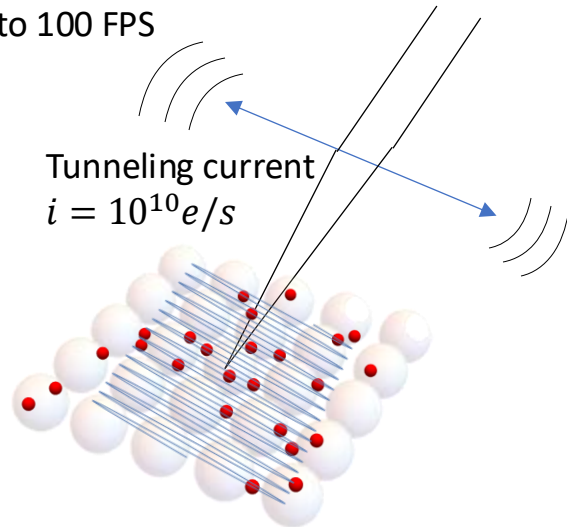
Simulation on D-Wave quantum annealer

$$H_S = -A(s) \sum_i \sigma_i^x / 2 + B(s) \left(\sum_{i < j} J_{i,j} \sigma_i^z \sigma_j^z + \sum_i h_i \sigma_i^z \right) / 2$$

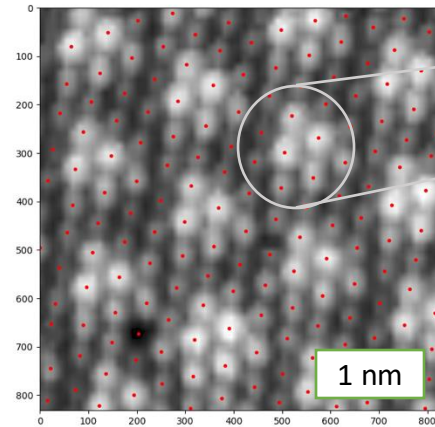
Fast-STM imaging of domain fluctuations in the H state of 1T-TaS₂

FAST scanning STM

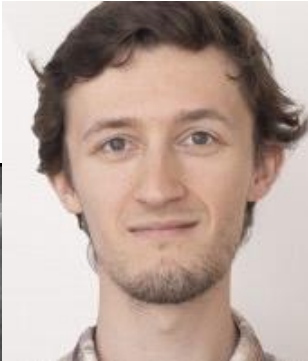
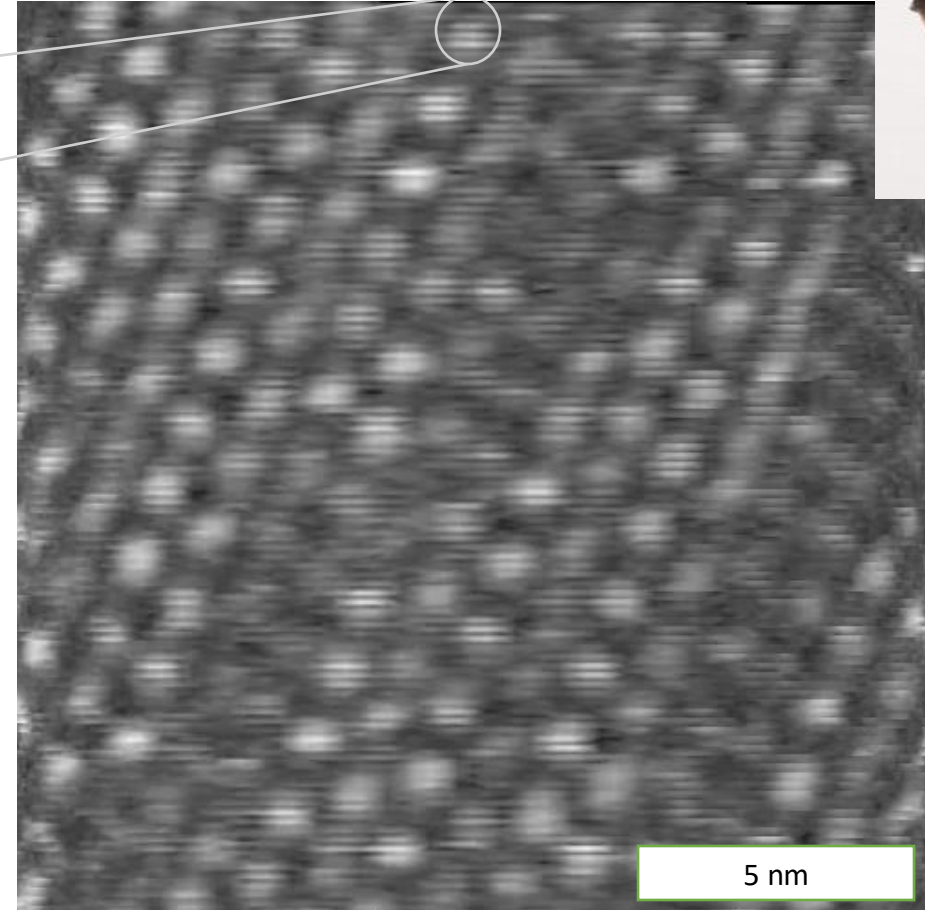
Up to 100 MHz sampling per pixel
up to 100 FPS



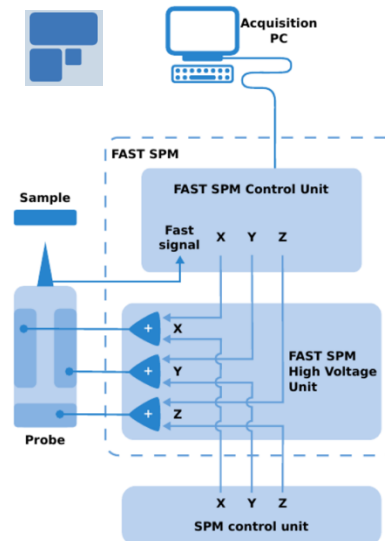
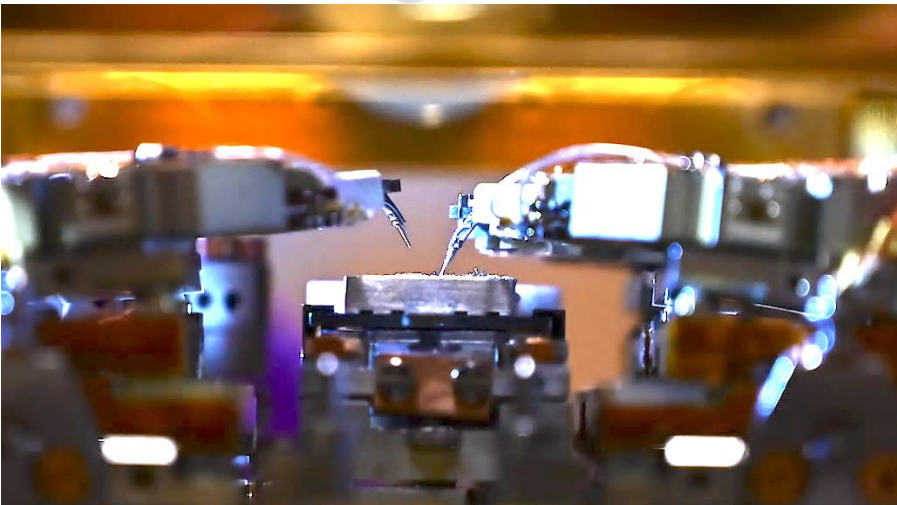
Atomic resolution



Raw real-time movie at 6 Hz framerate

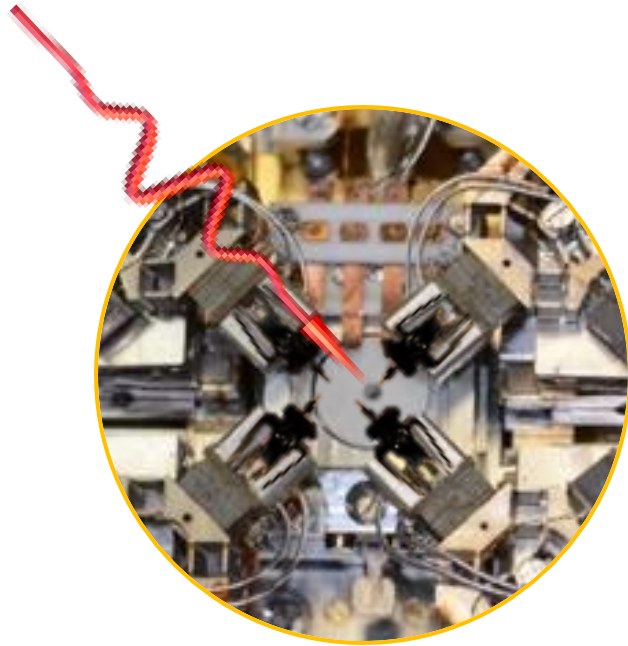


Yevhenii Vaskivskyi

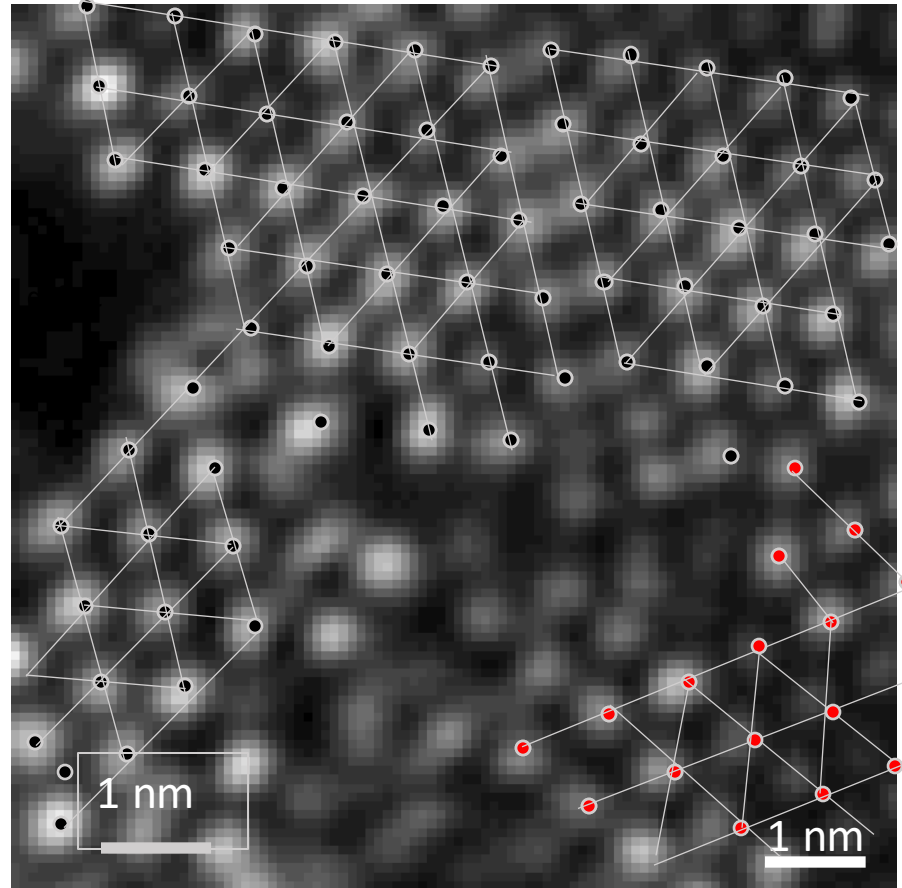


$$i = 1 \text{ nA}, V = 0.8 \text{ V}$$

A L-R domain vertex

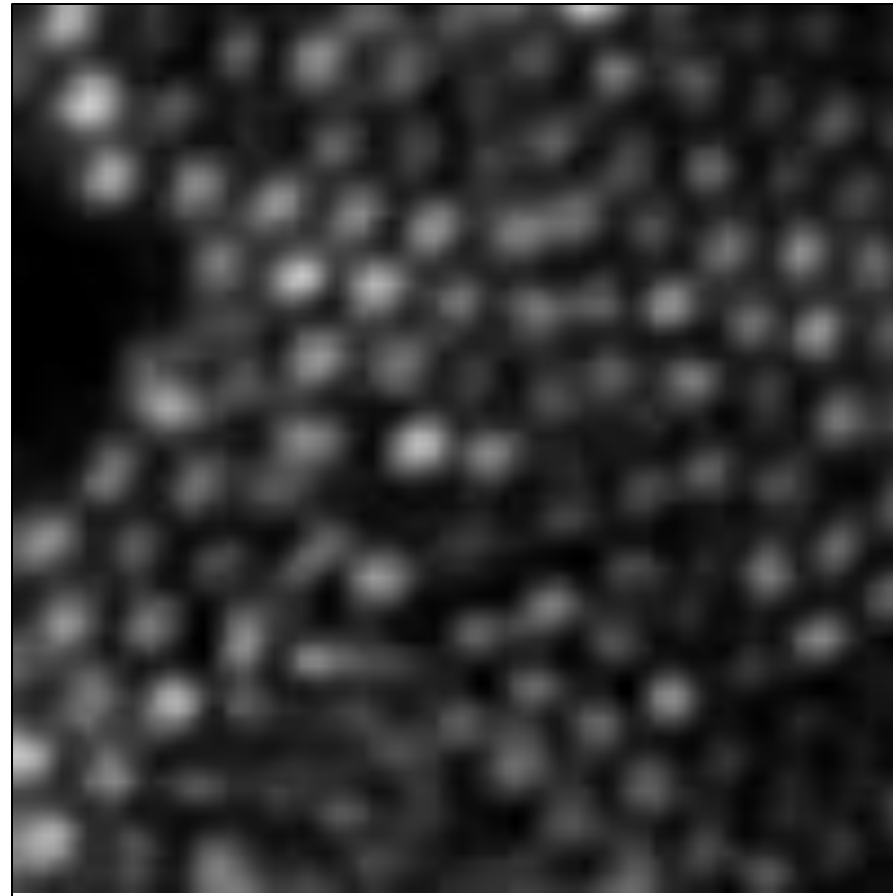


Quench



$i = 1 \text{ nA}, V = 0.8 \text{ V}$

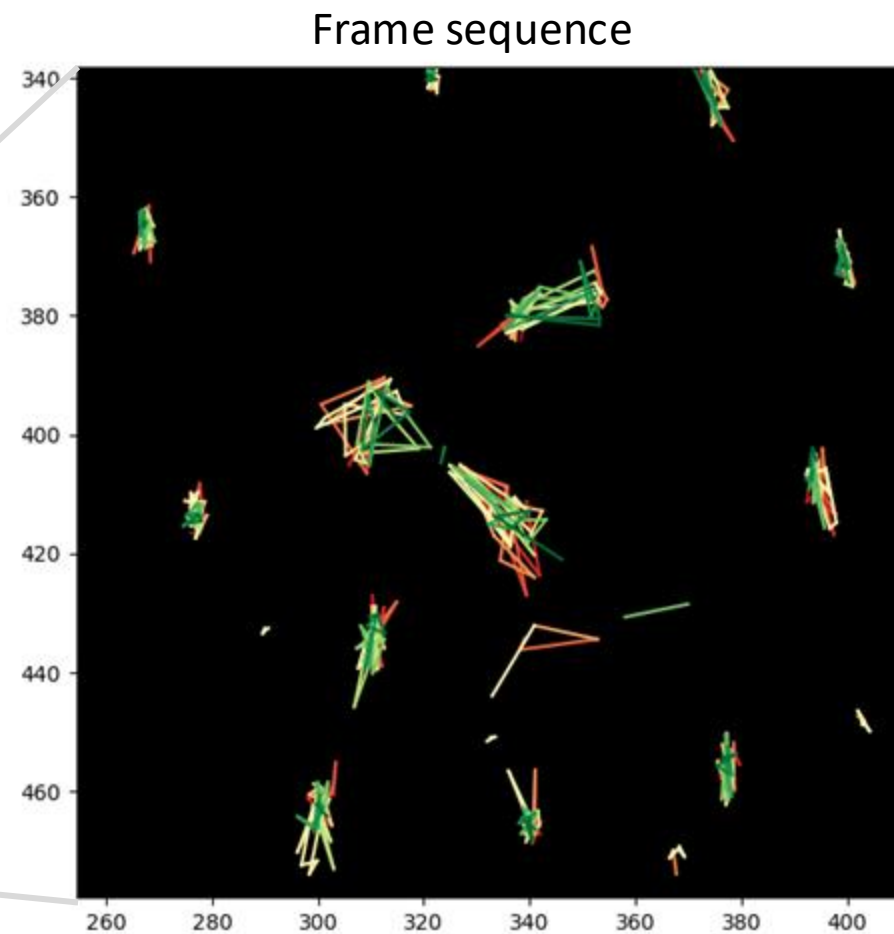
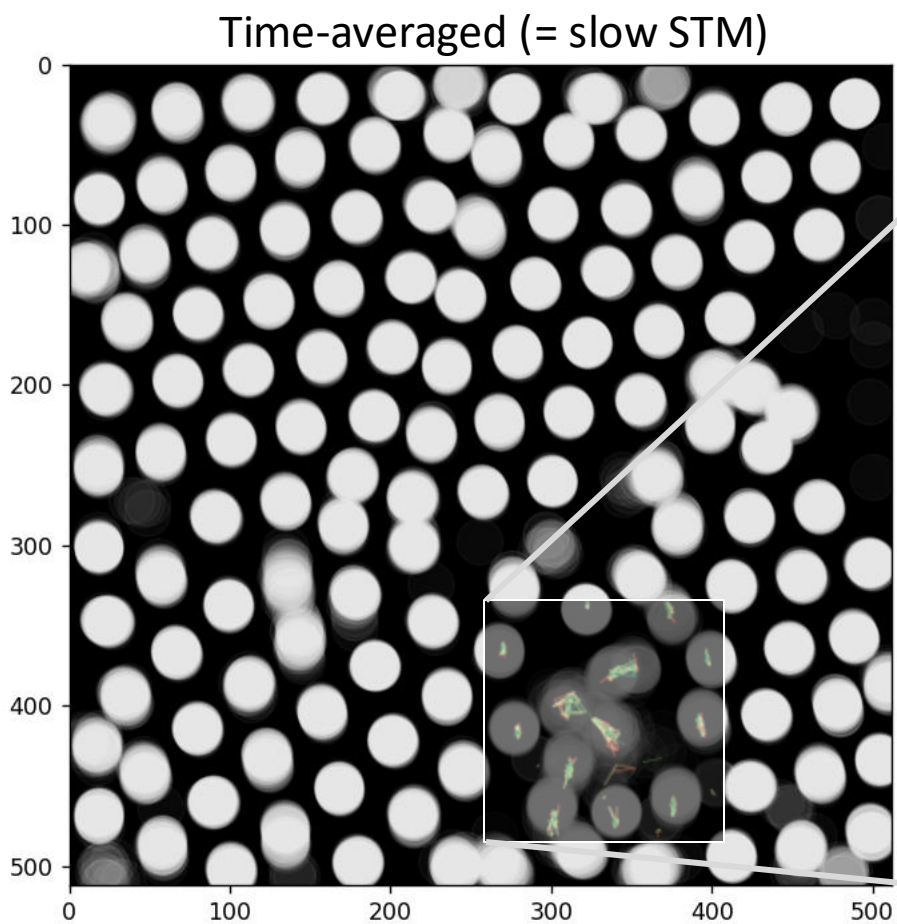
Fast STM polaron dynamics in real time



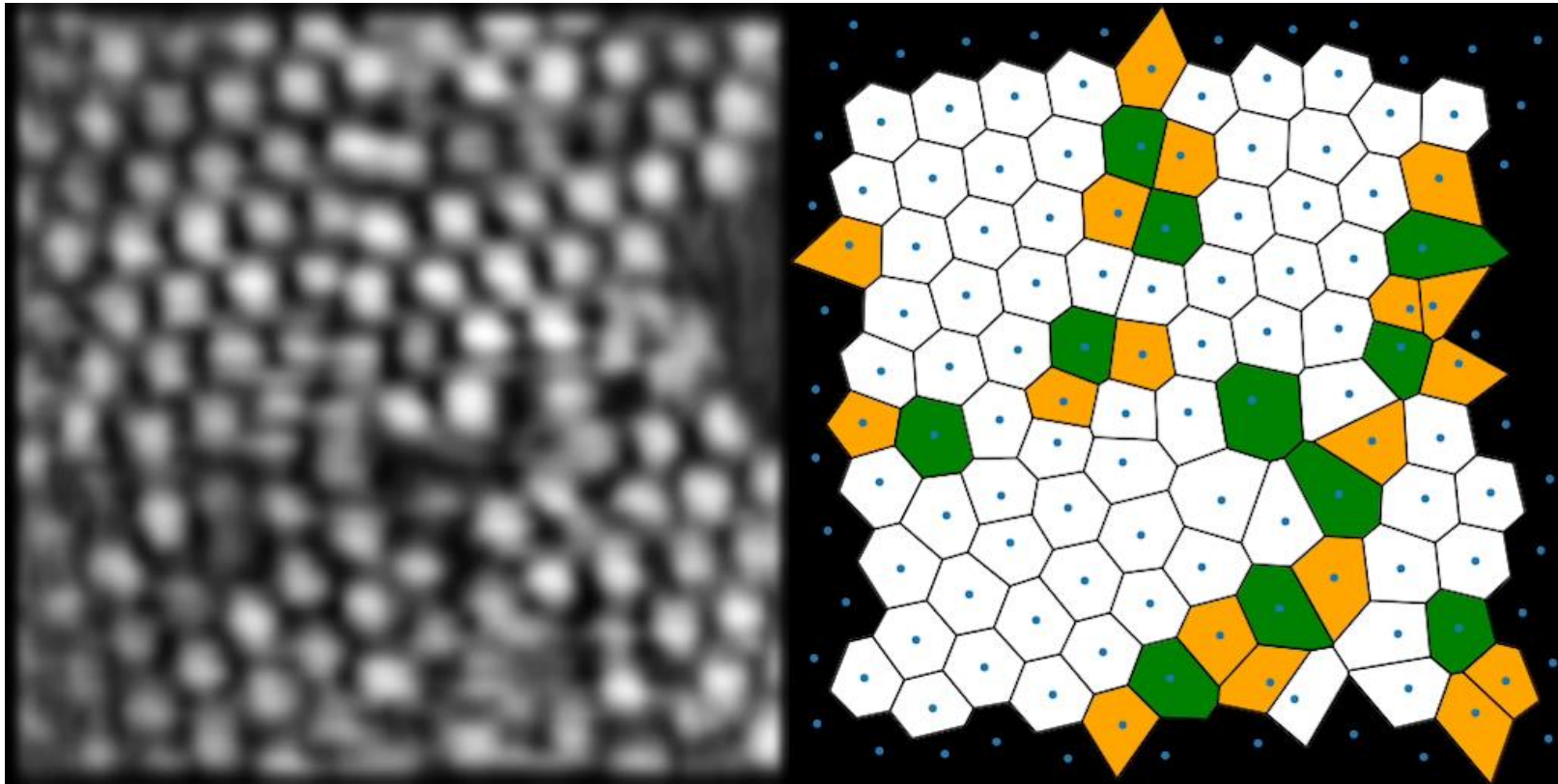
$i = 1 \text{ nA}, V = 0.8 \text{ V}$
 $T = 77 \text{ K}$

1T-TaS₂ 6 Hz STM real time video

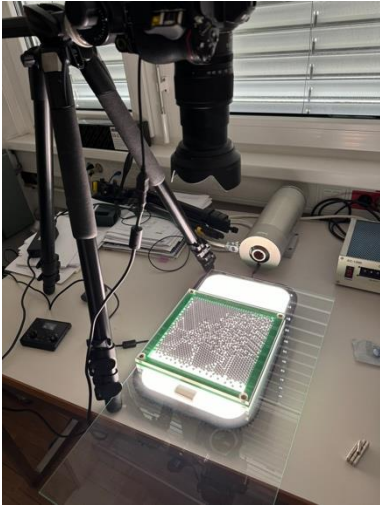
Electron 'trajectories'



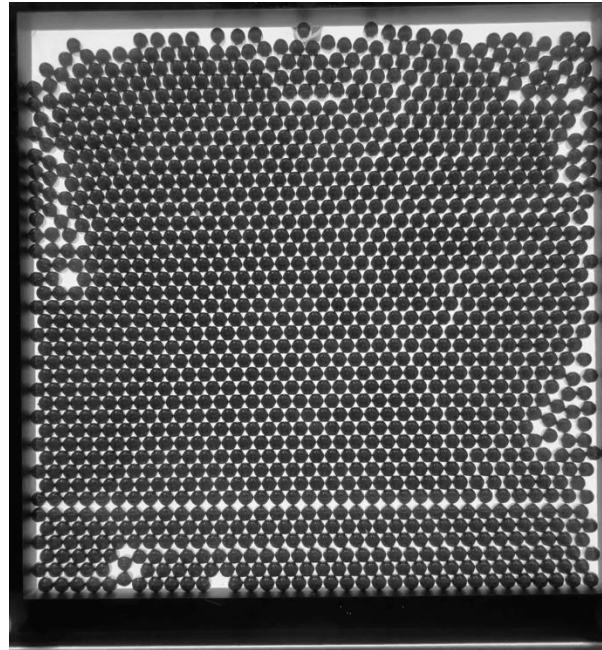
Tesselated Wigner-Seitz structure reveals motion of dislocations and disclinations



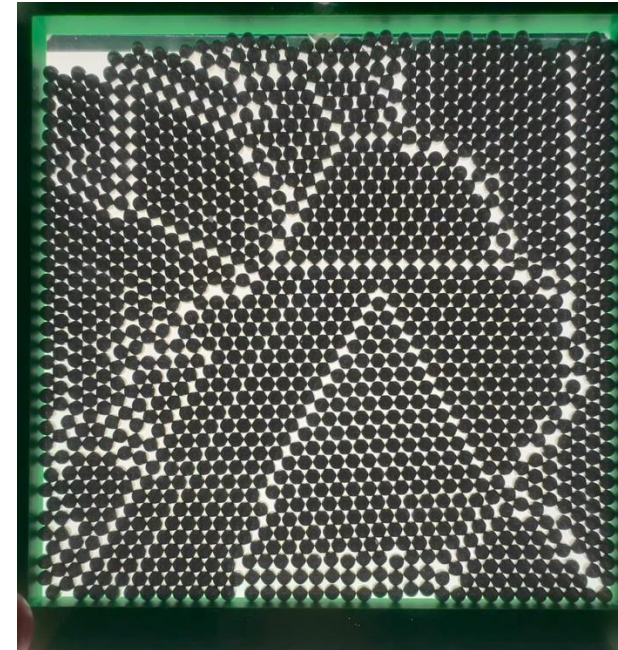
Classical packing in 2D – the effect of temperature and strain



Temperature (pseudorandom shaking)

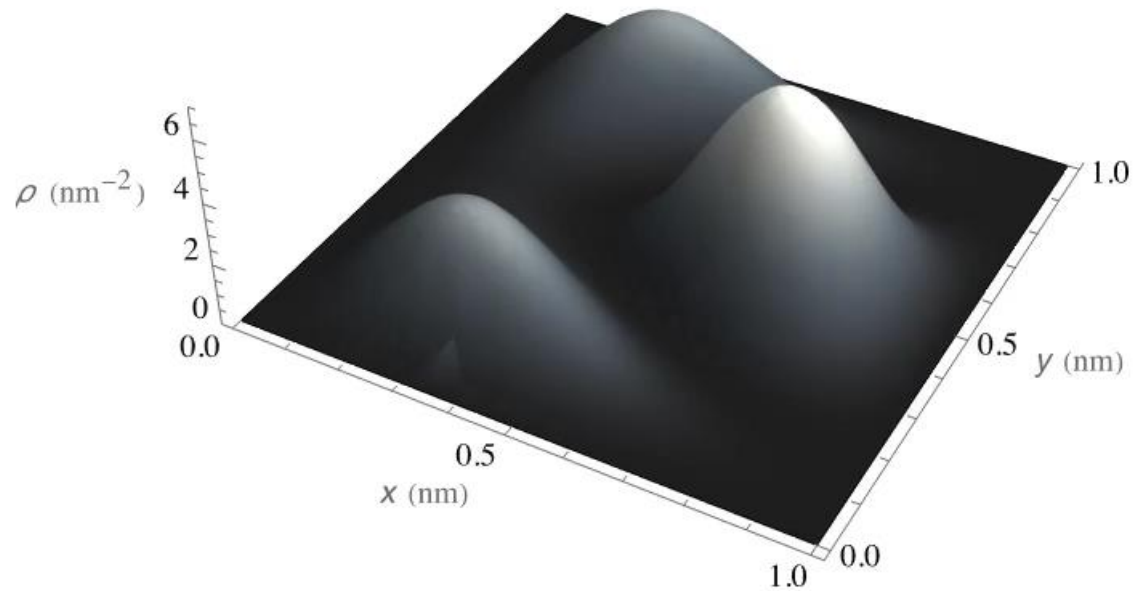


Jamming of steel balls under uniaxial pressure (gravity)



Non-interacting particle in a box

(time-dependent Schrödinger equation solution)



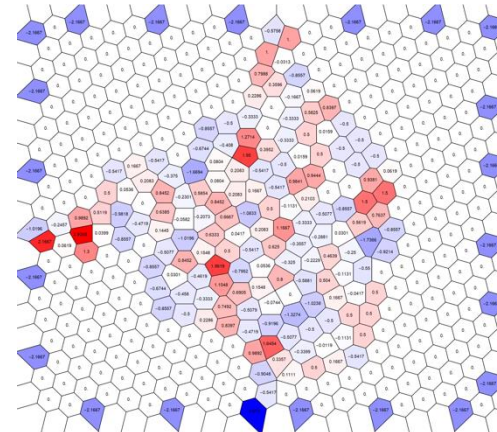
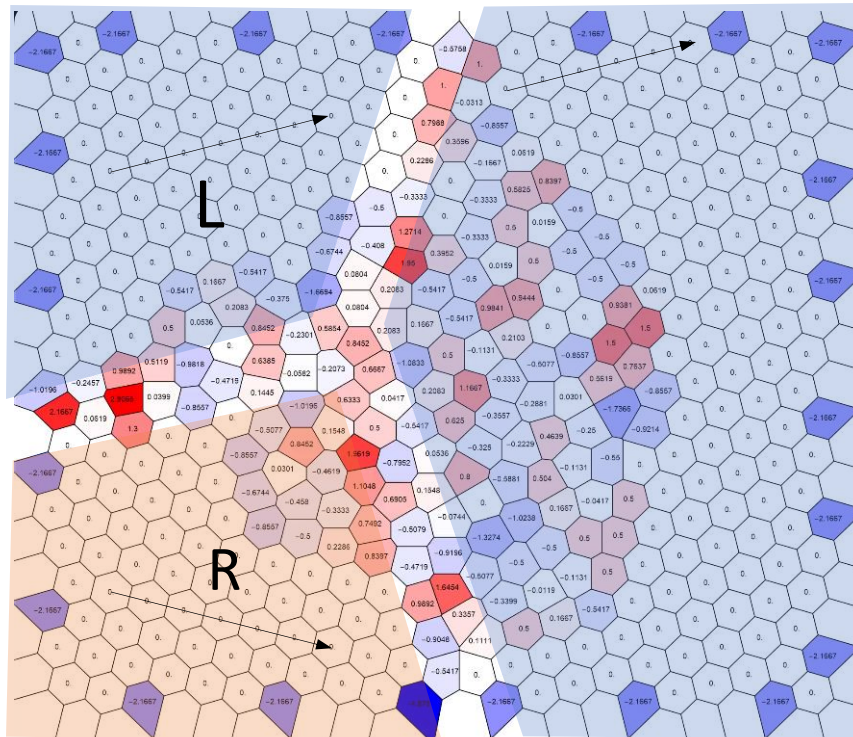
Timescale = 20 fs

$E_F = 1 \text{ eV}$

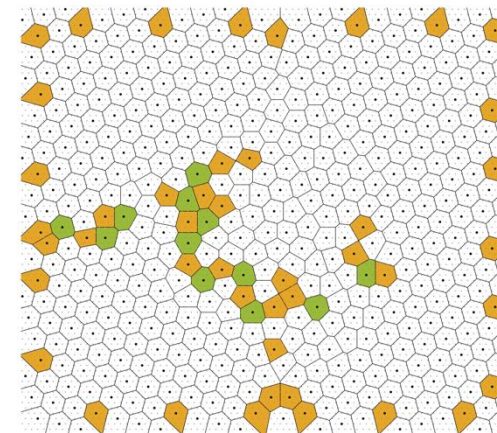
Model dynamics

$$\mathcal{H} = \sum_{i < j} V(i, j) n_i n_j,$$

Boundary conditions mimic the Fast STM experiment (L and R domains)

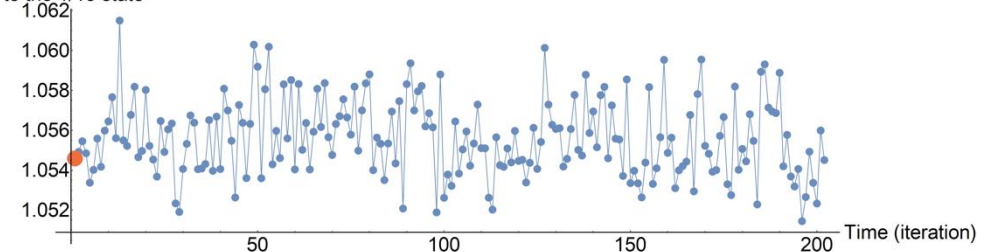


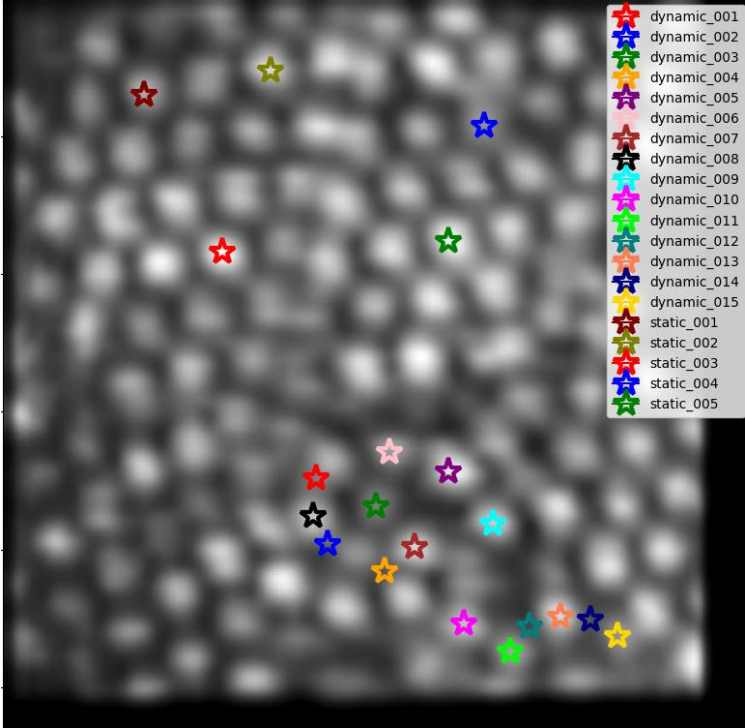
Charge density
(white is neutral $f=1/13$)



Defect density

Energy normalized
to the 1/13 state

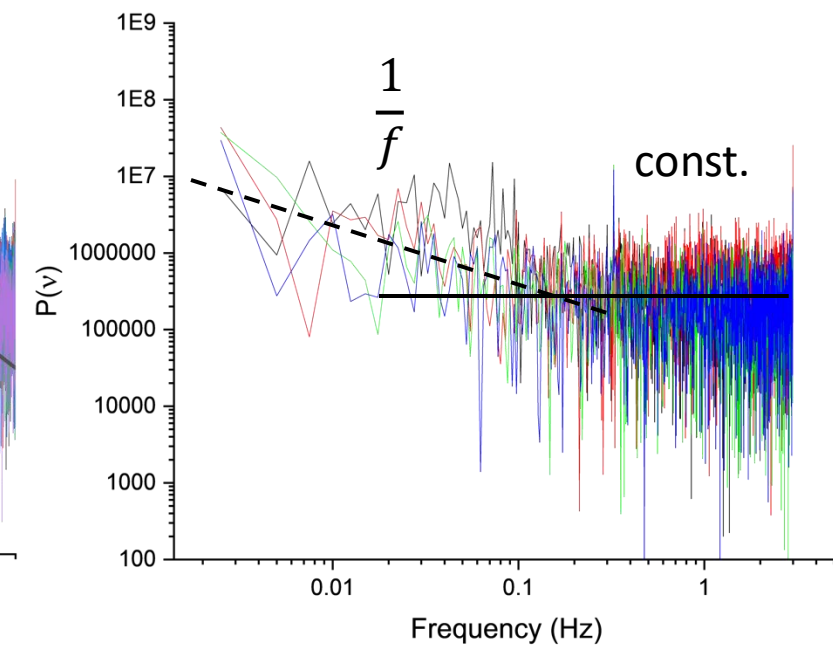
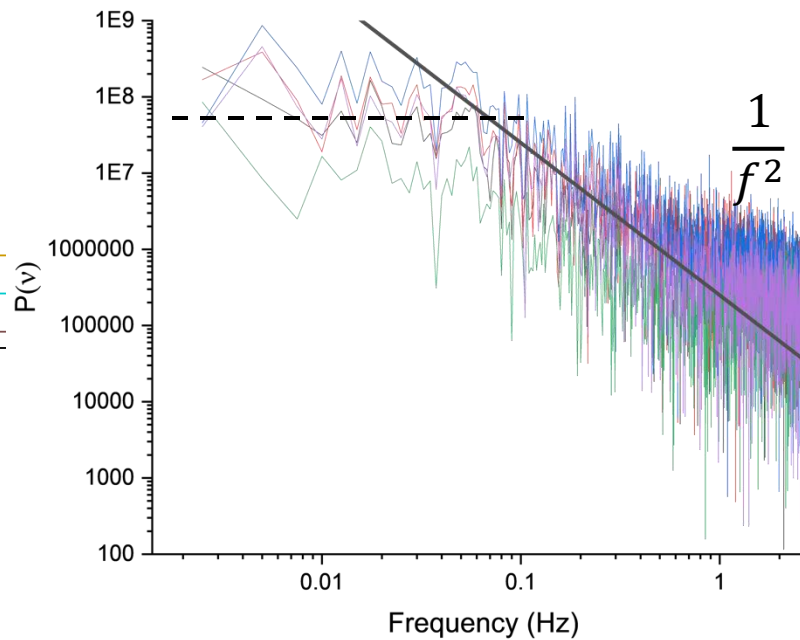
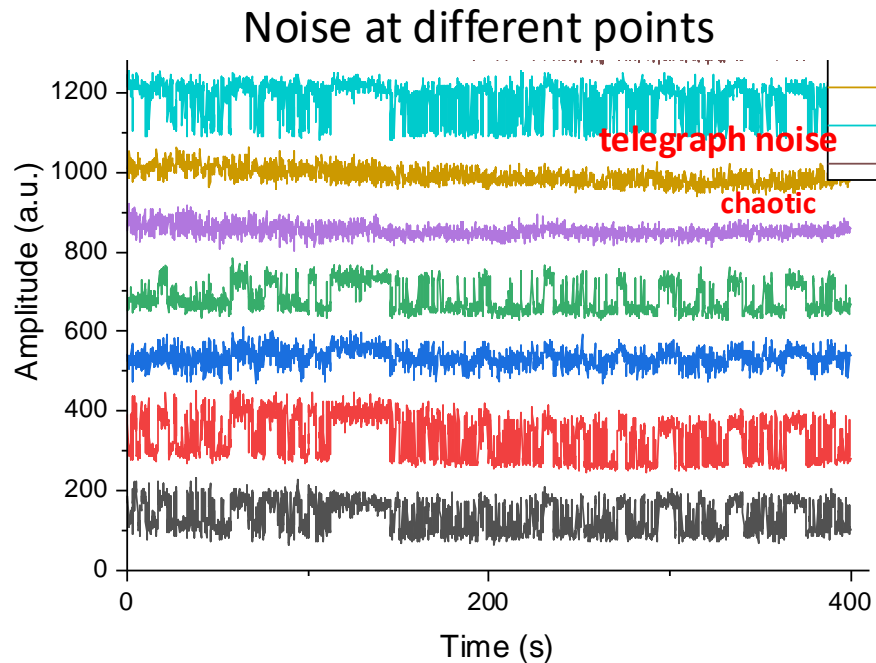




Noise analysis: 'telegraph noise' and chaotic dynamics observed at different points

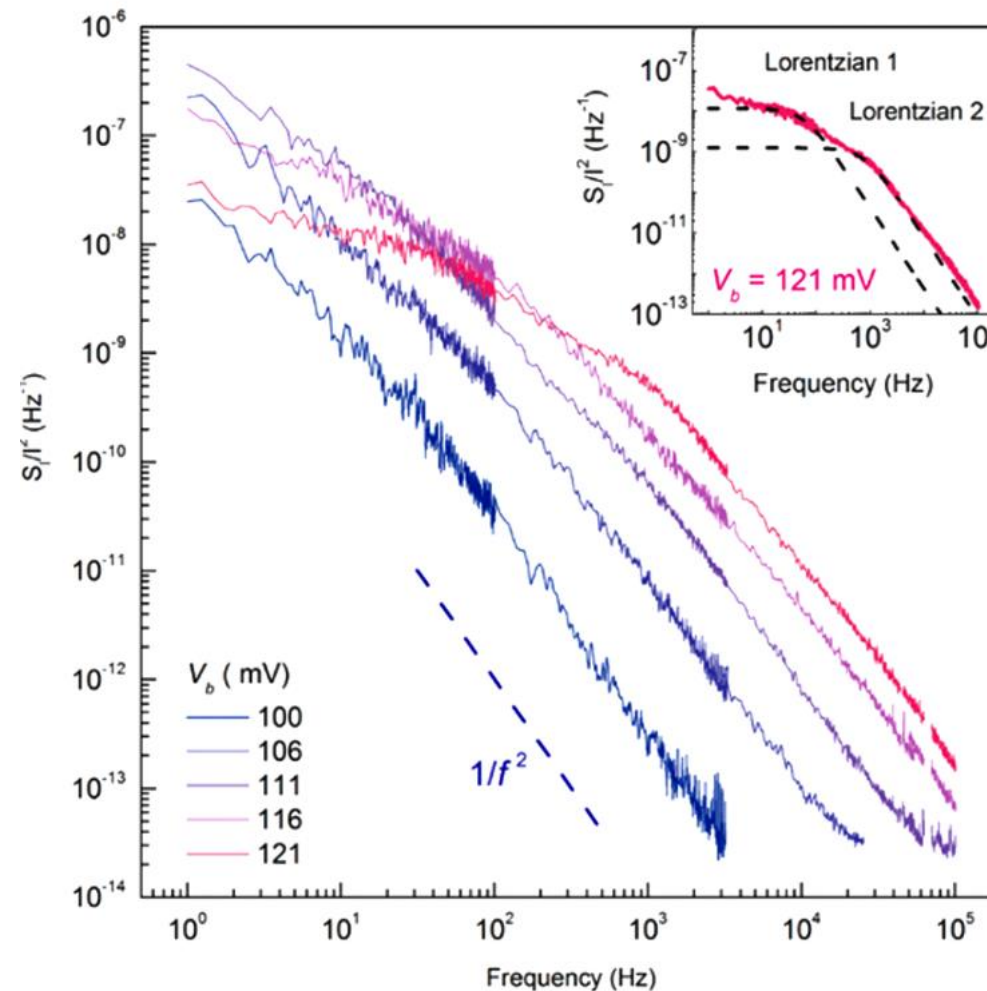
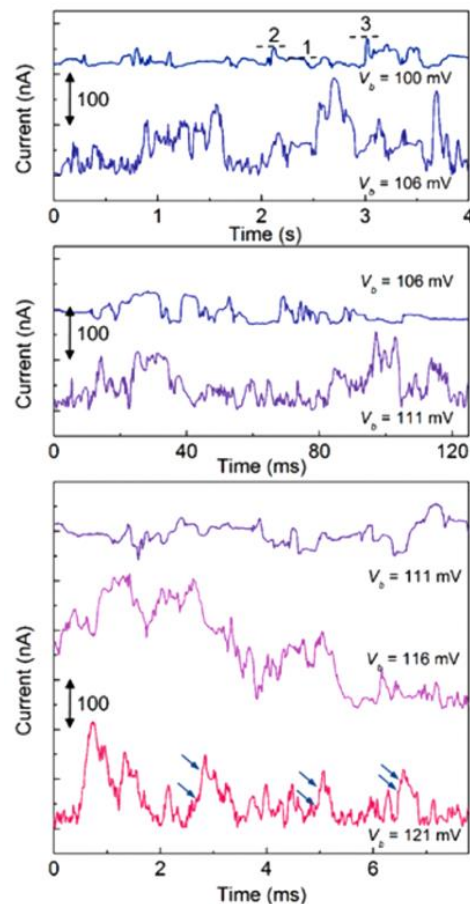
Dynamical point noise shows **telegraph noise**

Static point noise is **'chaotic'**

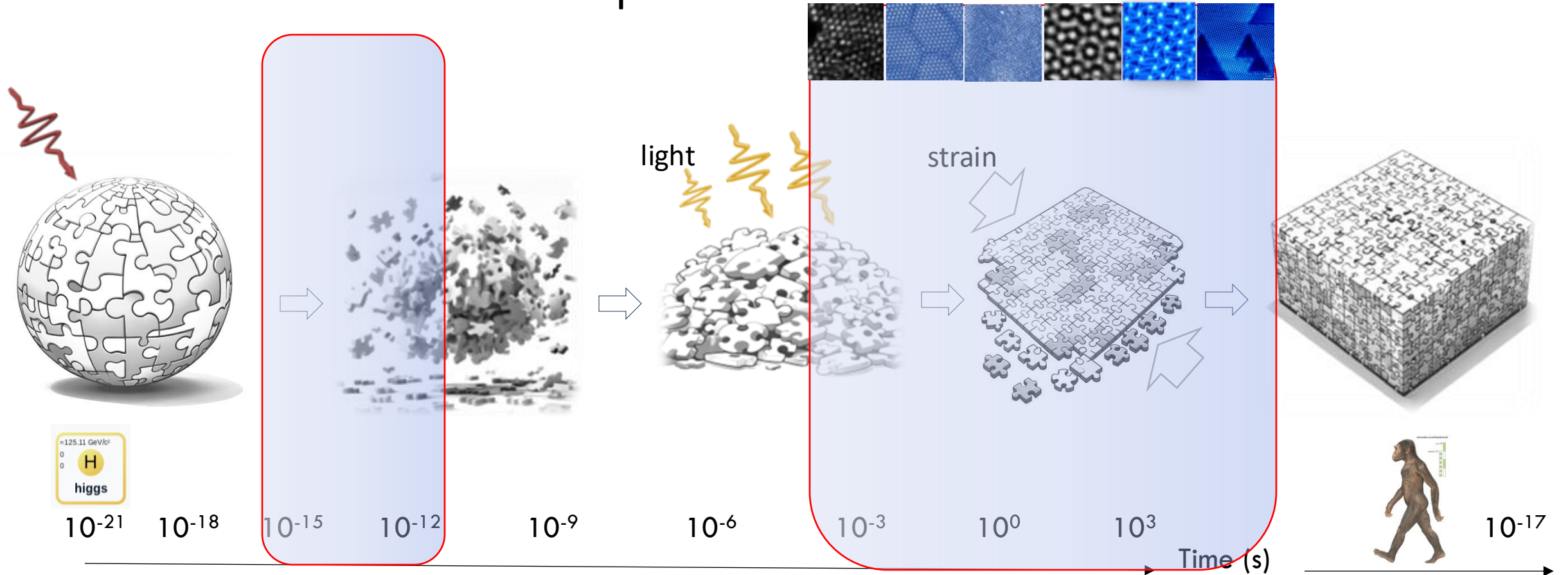


Low-Frequency Current Fluctuations and Sliding of the Charge Density Waves in Two-Dimensional Materials

Guanxiong Liu,[†] Sergey Rumyantsev,^{†,‡} Matthew A. Bloodgood,[§] Tina T. Salguero,^{§,¶} and Alexander A. Balandin^{*,†}



The aftermath of a phase transition



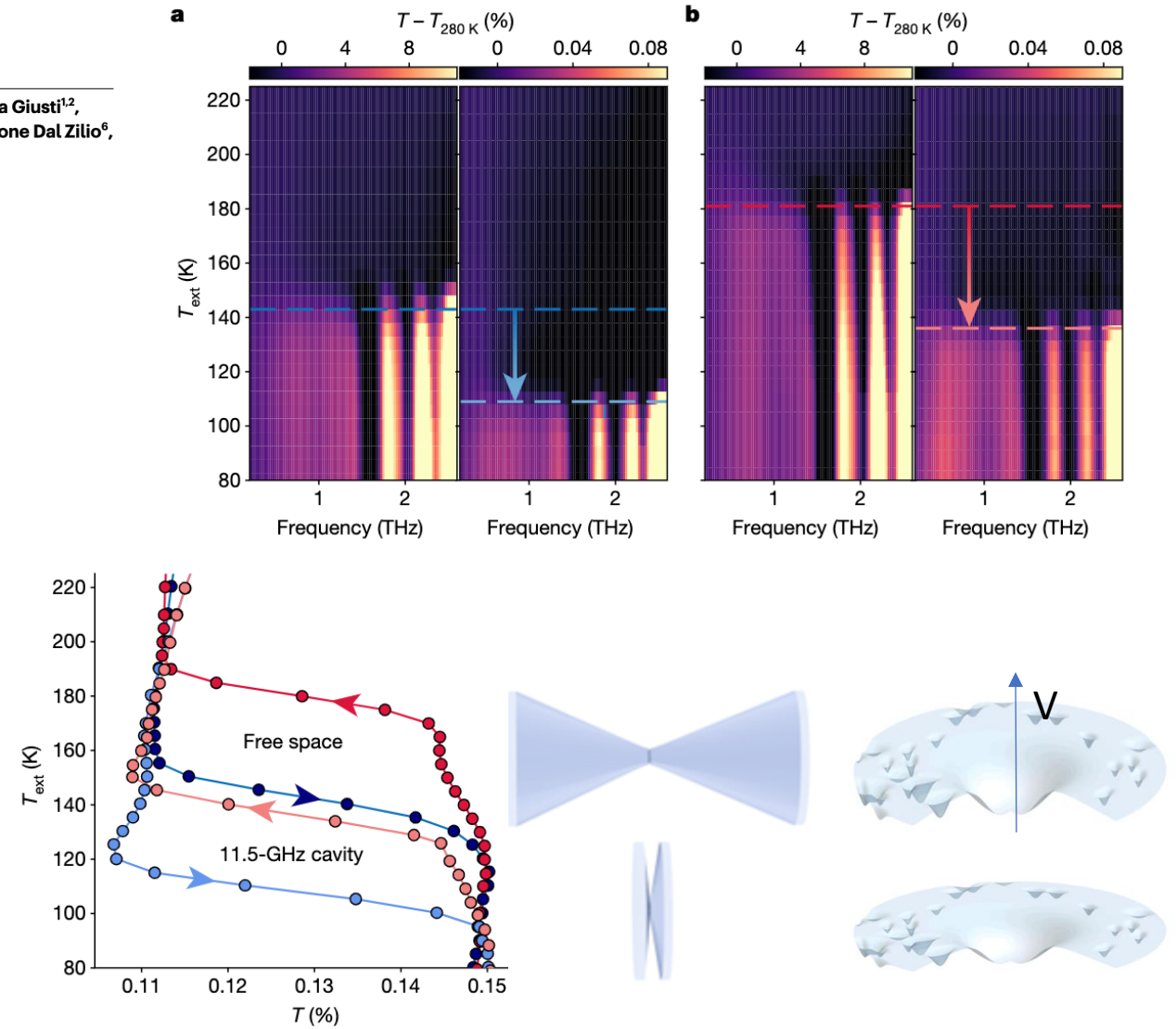
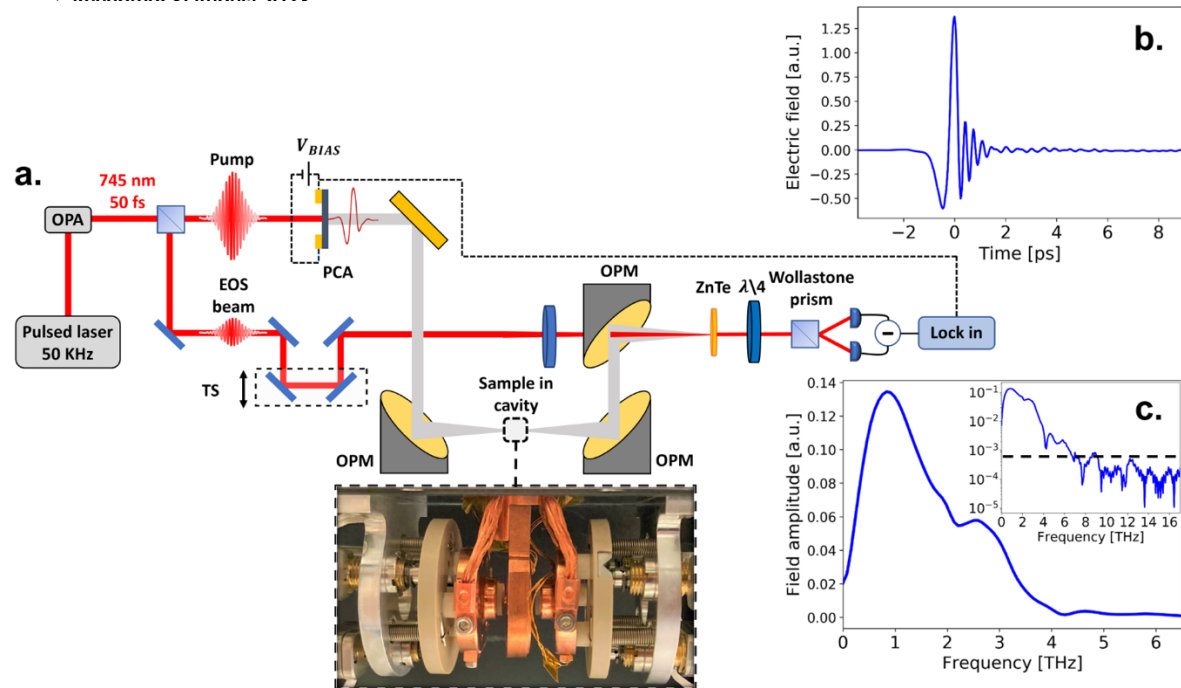
Cavity-mediated thermal control of metal-to-insulator transition in 1T-TaS₂

<https://doi.org/10.1038/s41586-023-06596-2>

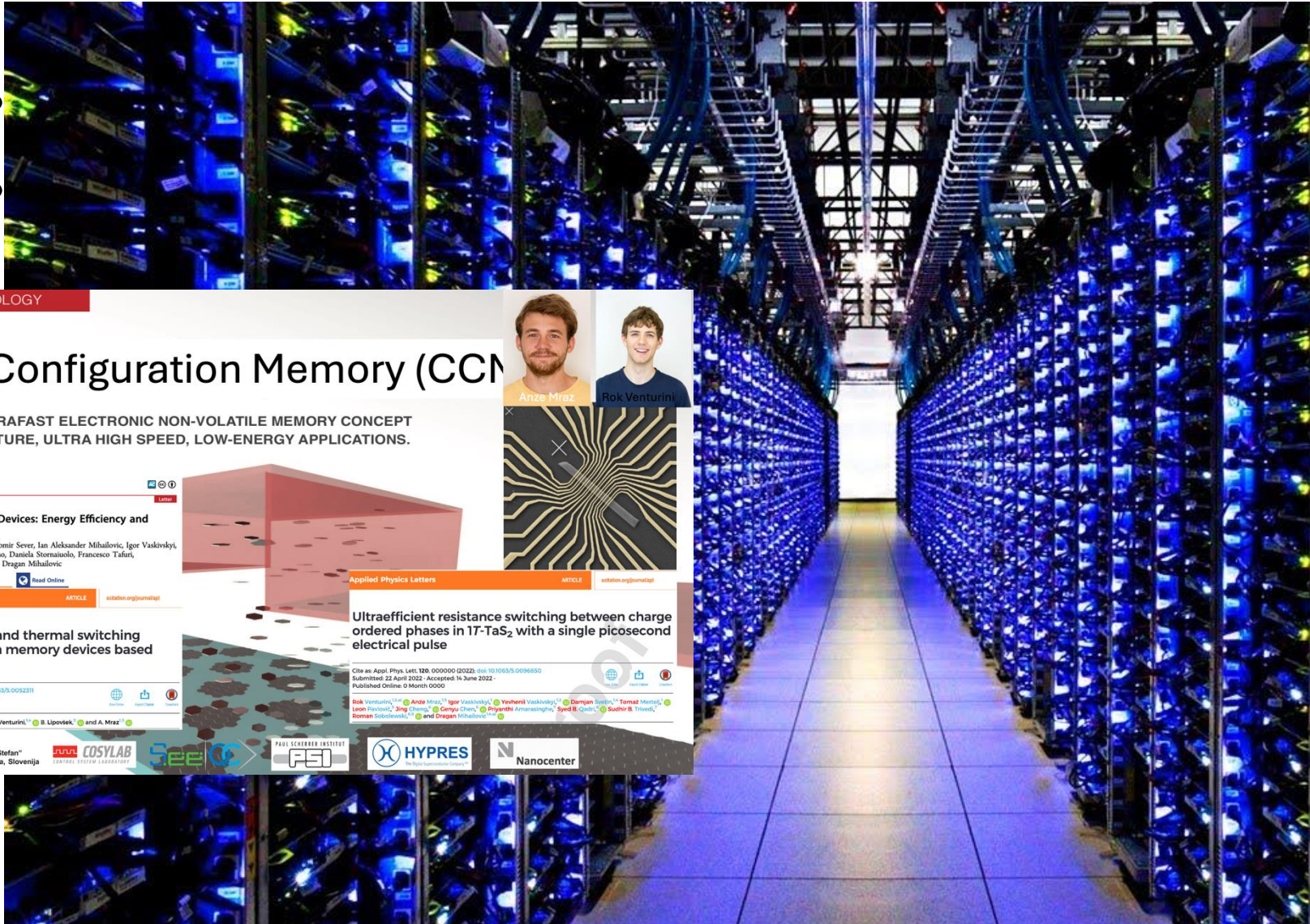
Received: 30 September 2022

Accepted: 21 August 2023

Giacomo Jarc^{1,2}, Shahla Yasmin Mathengatti^{1,2}, Angela Montanaro^{1,2,3}, Francesca Giusti^{1,2}, Enrico Maria Rigoni^{1,2}, Rudi Sergo², Francesca Fassioli^{3,4}, Stephan Winner⁵, Simone Dal Zilio⁶, Dragan Mihailovic⁷, Peter Prelovšek⁷, Martin Eckstein⁶ & Daniele Fausti^{1,2,3}✉



Metastable state devices



nature photonics

Article <https://doi.org/10.1038/s41566-024-01389-z>

A high-efficiency programmable modulator for extreme ultraviolet light with nanometre feature size based on an electronic phase transition

Received: 29 March 2023
Accepted: 9 January 2024
Published online: 02 February 2024

Igor Vaskivskiy^{1,2,3}, Anze Mrzaz^{1,2}, Rok Venturini^{1,3}, Gregor Jecel^{1,3}, Yevhenii Vaskivskiy^{1,3}, Riccardo Mincigrucci⁴, Laura Foglia⁴, Dario De Angelis⁴, Jacopo Stefano Pelli-Cresi⁴, Ettore Paltanin⁴, Danny Fainozzi⁴, Filippo Bencivenga⁴, Claudio Masciovecchio⁴ & Dragan Mihalovic^{1,5}

Check for updates

News & views

EUV photonics <https://doi.org/10.1038/s41566-024-01430-1>

Quantum materials offer modulator hope

Hermann A. Dürr

Check for updates

The diagram shows a 3D representation of a quantum material surface with a wavy, textured appearance. Several beams are shown interacting with the surface. An incident beam is labeled with wave vector k_1, ω_1 (write). A deflected beam is labeled with wave vector k_3, ω_3 . Another incident beam is labeled with wave vector k_2, ω_2 (write). A deflected beam is labeled with wave vector k_4, ω_4 . The deflected beams are collectively labeled as 'Deflected X-ray beam' and 'XUV beams'.

EMERGING TECHNOLOGY

Charge Configuration Memory (CCM)

AN 2-TERMINAL ULTRAFAST ELECTRONIC NON-VOLATILE MEMORY CONCEPT FOR LOW-TEMPERATURE, ULTRA HIGH SPEED, LOW-ENERGY APPLICATIONS.

NANO LETTERS

Charge Configuration Memory Devices: Energy Efficiency and Switching Speed

Anze Mrzaz^{*}, Rok Venturini, Damjan Svetin, Vitomir Sever, Ian Aleksander Mihalovic, Igor Vaskivskiy, Bojan Ambrozic, Goran Dražić, Maria D'Antonio, Daniela Stormaiuolo, Francesco Tafuri, Dimitrios Kazazis, Jan Ravnik, Yasin Ekinci, and Dragan Mihalovic

Cite this: <https://doi.org/10.1021/acs.nanolett.2c01116>

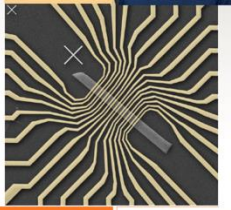
Applied Physics Letters

Ultrafast non-thermal and thermal switching in charge configuration memory devices based on 1T-TaS₂

Cite as: Appl. Phys. Lett. 119, 012306 (2021); doi:10.1063/1.5003231

Submitted: 30 March 2021 - Accepted: 31 May 2021 - Published Online: 8 July 2021

D. Mihalovic^{1,2*}, D. Svetin^{1,2}, I. Vaskivskiy^{1,2,3}, R. Venturini^{1,2,3}, B. Lipovsek^{1,2}, and A. Mrzaz^{1,2}



Applied Physics Letters

Ultraefficient resistance switching between charge ordered phases in 1T-TaS₂ with a single picosecond electrical pulse

Cite as: Appl. Phys. Lett. 120, 060601 (2022); doi:10.1063/1.5096850

Submitted: 22 April 2022 - Accepted: 14 June 2022 - Published Online: 6 Month 0000

Rok Venturini^{1,2,3*}, Anze Mrzaz^{1,2}, Igor Vaskivskiy^{1,2,3}, Yevhenii Vaskivskiy^{1,2,3}, Damjan Svetin^{1,2,3}, Tomaz Mertelj^{1,2,3}, Leon Pavlovic^{1,2,3}, Jing Chao⁴, Geyu Chen⁴, Priyankh Anandasingh⁴, Syed B. Qadir⁴, Sudhir B. Trivedi⁴, Roman Sobolewski⁴, and Dragan Mihalovic^{1,2,3}



Digital Coherent Control of a Superconducting Qubit

E. Leonard Jr.,^{1,†,‡} M. A. Beck,^{1,†,§} J. Nelson,^{2,¶} B.G. Christensen,¹ T. Thorbeck,^{1,§} C. Howington,²
 A. Opremcak,¹ I.V. Pechenezhskiy,^{1,||} K. Dodge,² N.P. Dupuis,^{1,**} M.D. Hutchings,^{2,††} J. Ku,²
 F. Schlenker,¹ J. Suttle,^{1,§} C. Wilen,¹ S. Zhu,¹ M.G. Vavilov,¹ B.L.T. Plourde,² and R. McDermott^{1,*}

¹*Department of Physics, University of Wisconsin-Madison, Madison, Wisconsin 53706, USA*

²*Department of Physics, Syracuse University, Syracuse, New York 13244, USA*

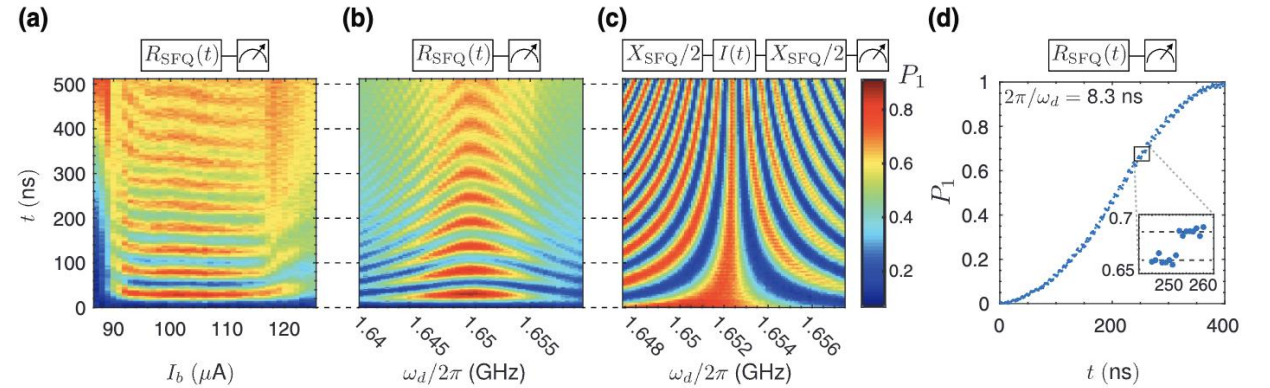
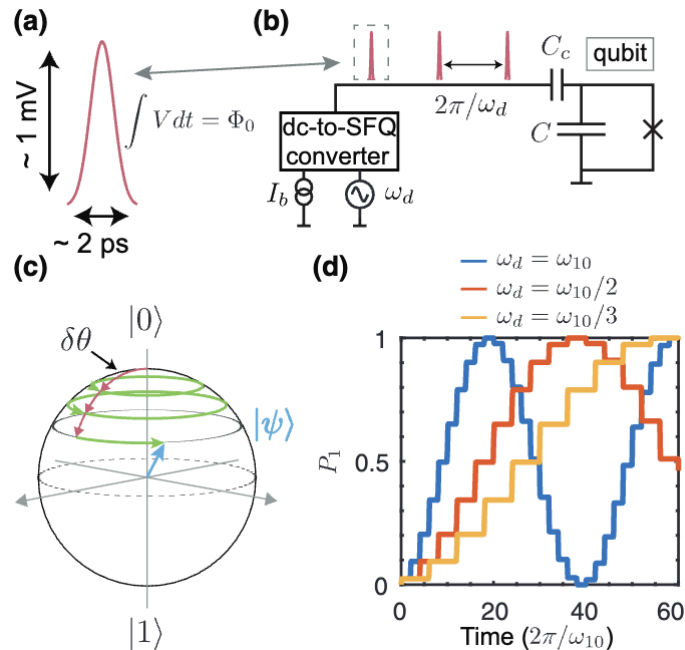
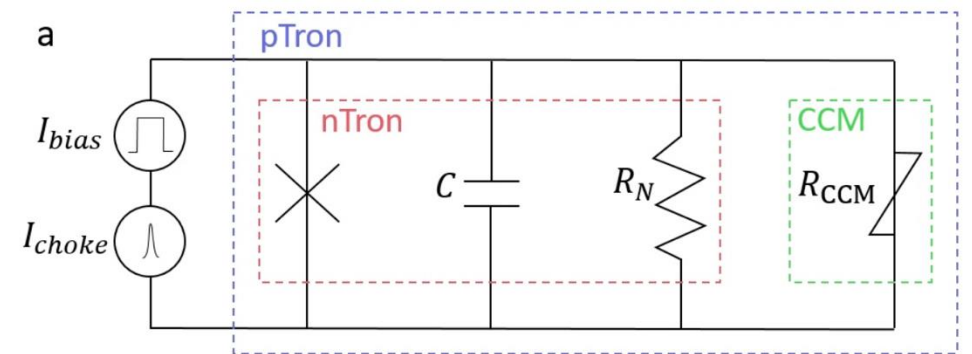
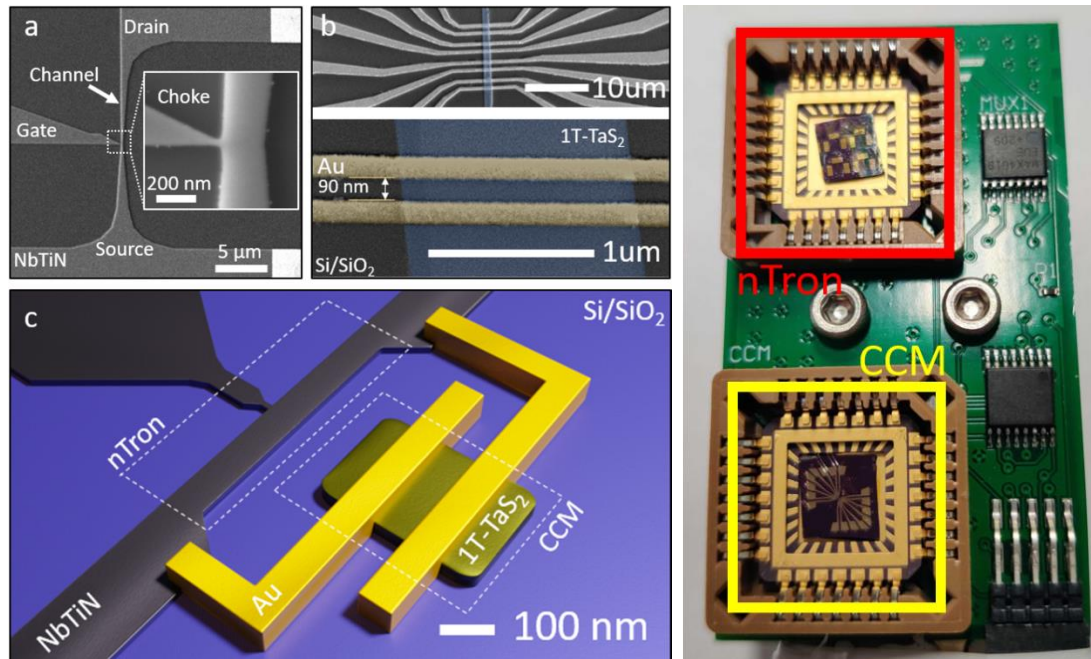


FIG. 3. Basic qubit operations driven by SFQ pulses. (a) SFQ-based Rabi oscillations as a function of bias current I_b to the SFQ driver circuit. Here, $\omega_d = \omega_{10}/3 \approx 1.65$ GHz. (b) Rabi chevron experiment and (c) Ramsey fringe experiment where the SFQ pulse frequency ω_d is varied slightly in the vicinity of $\omega_{10}/3$. (d) Time trace of a SFQ-based Rabi flop obtained with a pulse rate $\omega_{10}/41 = 120.90$ MHz. Inset: An enlargement of the discrete steps in $P_1(t)$ occurring every 8.3 ns, the SFQ pulse-to-pulse timing interval.

A CCM/superconductor hybrid memory device: The pTron (nTron amplifier and 1T-TaS₂ CCM)



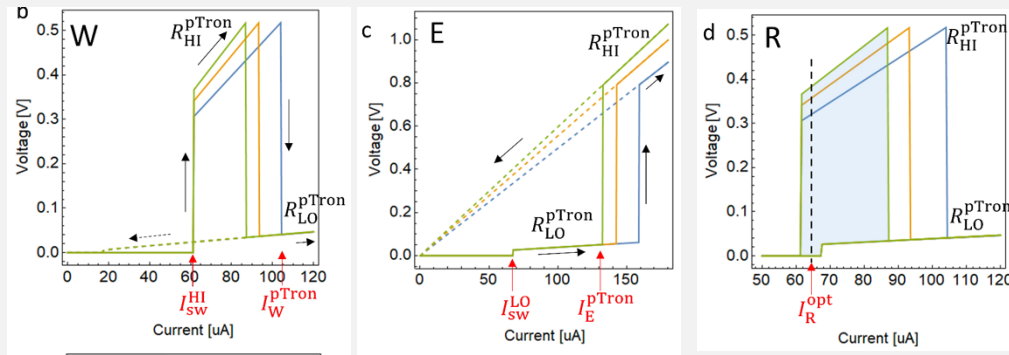
pTron equivalent circuit

Discrete implementation of nTron and CCM

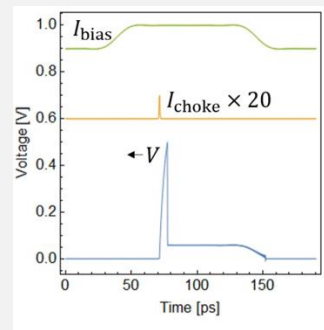
NB. NbTiN films were kindly provided by Wallraff's group (ETHZ)

pTron switching

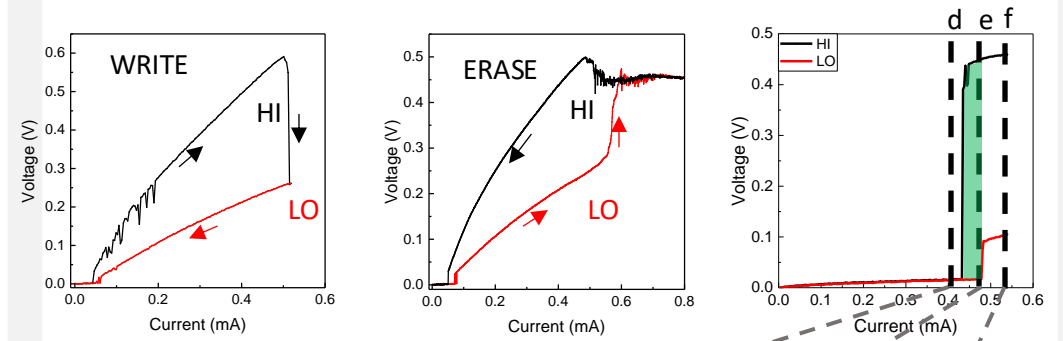
Model predictions



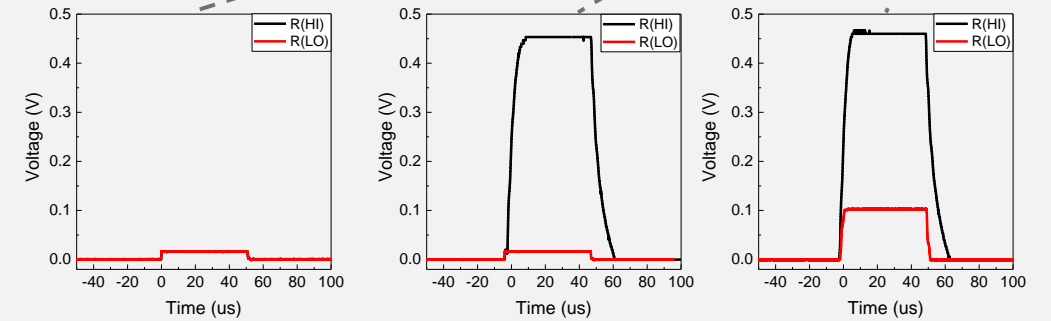
Time dynamics



Measured behaviour with NbTiN NW - CCMs



Readout



Acknowledgments

Jozef Stefan Institute

Yevhenii Vaskivskyi, Anže Mraz, Rok Venturini, Jaka Vodeb, Jan Ravnik, Yaroslav Gerasimenko, Michele Diego, Tomaz Mertelj, Igor Vaskivskyi, Denis Golež, Viktor Kabanov

PSI

Corinna Burri, Yasin Ekcinci, Dimitrios Kazazis, Simon Gerber, Jan Ravnik, Gabriel Aeppli

Elettra collaboration

Riccardo Mincigrucci, Filippo Bencivenga, Laura Foglia, Dario De Angelis, Jacopo-Stefano Pelli-Cresi, Ettore Paltanin, Danny Fainozzi, Claudio Masciovecchio

Cavity experiments

Giacomo Jarc, Shahla Yasmin Mathengattil, Angela Montanaro, Francesca Giusti, Enrico Maria Rigoni, Rudi Sergo, Francesca Fassioli, Stephan Winnerl, Simone Dal Zilio, Peter Prelovšek, Martin Eckstein, and Daniele Fausti

BNL

Emil Bozin

CNRS, Universite Paris Sud

Serguei Brazovskii

ETH

Andread Wallraff lab

Funding



UMEM4QC



HIMMS



Trajectory